The Pennsylvania State University

The Graduate School

College of Medicine

IMPACT OF HEART FAILURE AND OMECAMTIV MECARBIL ON BETA-CARDIAC MYOSIN FUNCTION

A Thesis in

Anatomy

by

Christopher M. Fetrow

Submitted in Partial Fulfillment
of the Requirements
for the Degree of

Master of Science

May 2016

The thesis of Christopher M. Fetrow was reviewed and approved* by the following:

Christopher Yengo
Associate Professor of Cellular and Molecular Physiology
Thesis Advisor

Patricia McLaughlin
Professor of Neural & Behavioral Sciences
Anatomy graduate program chair

Charles Lang
Distinguished Professor of Cellular and Molecular Physiology

*Signatures are on file in the Graduate School

Abstract

Purpose: Heart failure (HF) affects approximately 5.1 million people in the United States and is treated with a variety of drugs, many of which have long-term side effects such as cardiac arrhythmias. Due to a high mortality rate, it is important to find a drug that is more efficient and safe for long-term use. The small molecule cardiac myosin activator drug, omecamtiv mecarbil (OM), has been proposed as an effective treatment of heart failure. In this study we investigate the effects OM has on the interaction of actin and myosin.

Methods: Recombinant myosin was expressed in a C_2C_{12} expression system which was compared to myosin purified from human heart tissue provided by The University of Kentucky Biobank. We performed, *in vitro* motility and ATPase assays with and without OM to investigate the mechanisms of action of this drug. *In vitro* motility was obtained using fluorescent microscopy after fixing myosin to the surface of a microscope slide and inserting fluorescently labeled actin to create interaction with the surface attached myosin. The velocity, myosin density dependence, and actin filament length dependence were examined. ATPase assays were performed by examining actin-activated ATPase in the presence and absence of OM. The maximum ATPase rate (K_{cat}) and actin concentration at which the ATPase activity is ½ the maximum (K_{ATPase}) were obtained by plotting the ATPase activity as a function of actin concentration.

Results: ATPase assays showed there was a 6-fold decrease in the actin-activated ATPase rate. *In vitro* motility showed a 100-fold decrease in filament velocity and a small difference in length dependence with and without OM. Density dependence demonstrated that in the absence of

OM, velocity increased as the density of myosin was increased while the trend was the opposite in the presence of OM. Lastly, purified myosin from human heart tissue showed little movement in the absence of OM (3% filaments moving). However, the presence of OM dramatically increased the percentage of filaments moving (93%).

Conclusion: Based on our results, OM increased myosin's affinity for actin; however it remains unclear what the mechanism is behind the decrease in velocity in the *in vitro* motility assay. The decrease in sliding filament velocity may be detrimental to heart function and thus a therapeutic dose may need to be carefully chosen. Although the changes in the specific steps of the myosin ATP cycle are unclear, the enhanced interaction with actin in the presence of OM may increase force production in cardiac muscle.

Table of Contents

List of Figures

Abbreviations

ACC	American College of Cardiology
ADP	Adenosine Diphosphate
AHA	American Heart Association
Alexa	Fluorescent Label
ARVC	Arrythmogenic Right Ventricular Cardiomyopathy
ATP	Adenosine Triphosphate
B	Beta
BSA	Bovine Serum Albumin
Ca^{2+}	Calcium
C-AMP	Cyclic Adenosine Monophosphate
C_2C_{12}	Mouse Myoblast Cell Line
cMYBP-C	Cardiac Myosin Binding Protein
DCM	Dilated Cardiomyopathy
DMSO	Dimethyl Sulfoxide
DTT	Dithiothreitol
ECG	Electrocardiogram
EGTA	Ethylene Glycol Tetracetic Acid
ESV	End Systolic Volume
F	Fahrenheit
F-Actin	Filamentous Actin

GOC	Glucose Oxidase Catalase
HCM	Hypertrophic Cardiomyopathy
HF	Heart Failure
HMM	Heavy Meromyosin
K_{ATPase}	½ Maximum ATPase Rate
K_{cat}	Maximum ATPase Rate
KCl	Potassium Chloride
kD	Kilodalton
Kg	Kilogram
LDH	Lactate Dehydrogenase
LVAD	Left Ventricular Assistive Device
M2B	β Cardiac Myosin
Mg	Milligram
$MgCl_2$	Magnesium Chloride
mL	Milliliter
mM	Millimolar
MOPS	Morpholinopropane Sulfonic Acid
NADH/NAD	Nicotinamide Adenine Dinucleotide
Ng	Nanogram
Nm	Nanometers
OM	Omecamtiv Mecarbil
PEP	Phosphoenolpyruvate Carboxylase

P_i	Inorganic Phosphate
Sec	Seconds
SV	Stroke Volume
µl	Microliter
µM	Micromolar

Acknowledgements

I want to acknowledge the guidance of my thesis research advisor Dr. Christopher Yengo and the support I was given by the Yengo Lab. I would also like to thank my committee members Dr. Patricia McLaughlin and Dr. Charles Lang for their feedback and assistance with my research project.

Chapter 1: Introduction

1.1 Epidemiology of Heart Failure

1.1.1 Prevalence of Heart Failure

Heart failure (HF) is a chronic, progressive condition in which the heart muscle is unable to pump enough blood to meet the body's needs for nutrients and oxygen. Failure of the heart can also be thought of as a problem with lack of efficiency. Systolic heart failure is a condition when the left ventricle muscle cannot efficiently pump blood out of the heart. Diastolic heart failure has been identified as one of the possible causes of systolic heart failure by characteristically failing to fill the heart up with blood (American Heart Association, 2015). Both systolic and diastolic heart failure yield the heart unable to keep up with the work load which results in the heart trying to overcompensate by remodeling.

According to the CDC, 5.1 million people in America are affected by heart failure (National Center for Chronic Disease Prevention and Health Promotion, 2015). Additionally, an estimated 400,000 to 700,000 new cases of heart failure are diagnosed each year. Patients experience a buildup of blood and fluid in the lungs, fluid in lower extremities (edema) and tiredness with shortness of breath as a result of the heart's inefficiency to pump blood (Heart Failure Society of America Inc., 2015). The total number of inpatient cardiovascular operations and procedures increased 28%, from 5,939,000 in 2000 to 7,588,000 in 2010 (Mozaffarian et al., 2013). Though most of these hospitalizations were individuals ages 65 and over, the portion of

hospitalizations for those under age 65 increased from 23% to 29% over this time period (National Center for Chronic Disease Prevention and Health Promotion, 2015).

1.1.2 Costs and Outcomes Associated with Heart Failure

According to the CDC, one in 9 deaths in 2009 included heart failure as a contributing cause while about half of the people who develop heart failure die within 5 years of diagnosis (National Center for Chronic Disease Prevention and Health Promotion, 2015). This prognosis is worse than many of the most common cancer diagnoses (Stewart et al., 2001). Immediate outcomes require a drastic lifestyle change which includes diet maintenance, moderation of physical exertion and administration of daily medications. In the United States, the annual cost of heart failure in 2010 was estimated to be $39.2 billion or approximately 2% of the total US health-care budget. The cost per patient diagnosed with heart failure is associated with annual costs of approximately $8500 according to data from the National Heart and Lung Institute cardiovascular health study (Braunschweig, 2011). These estimates are hypothesized to be somewhat low because the annual costs per patient is only evaluated by the National Heart and Lung Institute if the primary diagnosis or cause of death is Heart Failure.

Heart failure is considered an epidemic condition that is expected to grow exponentially assuming that more effective treatments are not found. The American Heart Association forecasts that by 2030, greater than 8 million people in the United States (1 in every 33) will develop heart failure. Between 2012 and 2030, the total direct medical costs of heart failure are projected to increase from $21 billion to $53 billion, and the total costs including indirect

costs for heart failure, are estimated to increase from $31 billion in 2012 to $70 billion in 2030 (Heidenreich et al., 2013).

1.1.3 Causes of Heart Failure

One of the main causes of heart failure is coronary heart disease. This condition is the most common cause of death in the general population and is characterized by atherosclerosis, plaque buildup in the arteries that supply blood to the heart (Mann, 2011). In coronary artery disease the plaques prevent adequate blood flow and result in ischemia to the surrounding cardiac muscle tissue. This will then lead to cardiac muscle cell death which will affect contractile function. The reduction in functional cardiac muscle can lead to a reduced cardiac output as a result of contractile changes within the heart.

Additionally, genetic disorders can play an important role in the development of contractile abnormalities which lead to heart failure and/or cardiomyopathies. Genetic mutations in many of the contractile proteins of the heart can contribute to the various pathologies of HF by altering the structure and function of the contractile proteins. The genes causing different types of cardiomyopathy overlap to a large extent, and mutations in the same gene may exert opposite functional effects. It is unknown how variations in a single gene generates different cardiomyopathic phenotypes; however, current hypotheses under investigation include transcriptional regulation, RNA turnover, gene modification and environmental influences (Yang et al., 2015).

There are three major types of inherited cardiomyopathies which include hypertrophic cardiomyopathy (HCM), dilated cardiomyopathy (DCM), and arrhythmogenic right ventricular cardiomyopathy (ARVC). Arrhythmogenic right ventricular cardiomyopathies are characterized by the replacement of muscle tissue with scar and fat tissue as a result of injury to the myocardium and can be characterized as biventricular or left dominant conditions. Hypertrophic cardiomyopathies are identified by their thick muscular walls (myocardium) which diminish space in the chamber of the left ventricle. Dilated cardiomyopathies differ from hypertrophic cardiomyopathies because they are characterized by thin myocardial walls and therefore have enlarged chambers (Spudich, 2014). Currently, there are more than 40 gene mutations that have been implicated in the development of DCM. The majority of cardiomyopathies are inherited, autosomal dominant, gene mutations (Garcia-Pavia et al., 2013). More specifically, there have been over 250 different genetic mutations identified that are responsible for cardiomyopathy development in β-cardiac myosin alone (Aksel, 2015).

Hypertrophic is the most common cardiomyopathy seen in heart failure patients, affecting approximately 1 in 500 people, and is thought to be caused by compensatory remodeling of the heart (Spudich, 2014). Because of the increase in heart muscle and extracellular matrix, the heart becomes stiffer which leads to the requirement of higher blood pressure within the chamber to contract the ventricle. Hypertrophic cardiomyopathies can be developed by inheritance of mutated genes which myofilament proteins of the sarcomere, Z-disc proteins, Ca2+-handling proteins, and other proteins related to the sarcomere (Garcia-Pavia et al., 2013). Hypertrophic cardiomyopathies are difficult to diagnose early due to mild

symptoms and the inability to visualize heart remodeling in early stages of heart failure (McKenna & Elliot, 2014).

1.2 Anatomy of the Heart

1.2.1 Heart Chambers

Although the heart starts off as a single tube in the early prenatal stages of human life, it develops multiple chambers as the embryo develops. In general, the heart can be pictured as a pair of valved muscular pumps combined in a single organ separated into "right" and "left" hearts. Built within the two pumps, there are four chambers consisting of left and right atria and left and right ventricles. The two atria receive venous blood and use weak contractile forces to fill the ventricles. The ventricles use heavy expulsive contractions to force blood into the main arterial trunks which soon after is sent systemically (Standring, 2008).

The "right" heart is composed of the right atrium which receives venous blood from the superior and inferior vena cava along with the main venous inflow from the heart itself via the right coronary sinus. The venous blood continues to travel through the atrioventricular orifice by passing through the tricuspid valve into the right ventricle. The blood is next ejected into the pulmonary trunk to enter the lungs where it is oxygenated. The "left" heart is composed of the left atrium which receives all of the pulmonary inflow of oxygenated blood as well as a small amount coronary venous blood. Similarly to the right atrium, the left atrium contracts to push the blood through the mitral valve (Standring, 2008). The left ventricle is positioned in anterior to the left atrium in which blood flows in towards its apex (Rosse, 1997). Upon

contraction of the left ventricle, pressure builds closing the mitral valve to prevent backflow, propelling blood to the aortic sinuses and the ascending aorta. At this point, the blood is distributed to the systemic circulation (Standring, 2008).

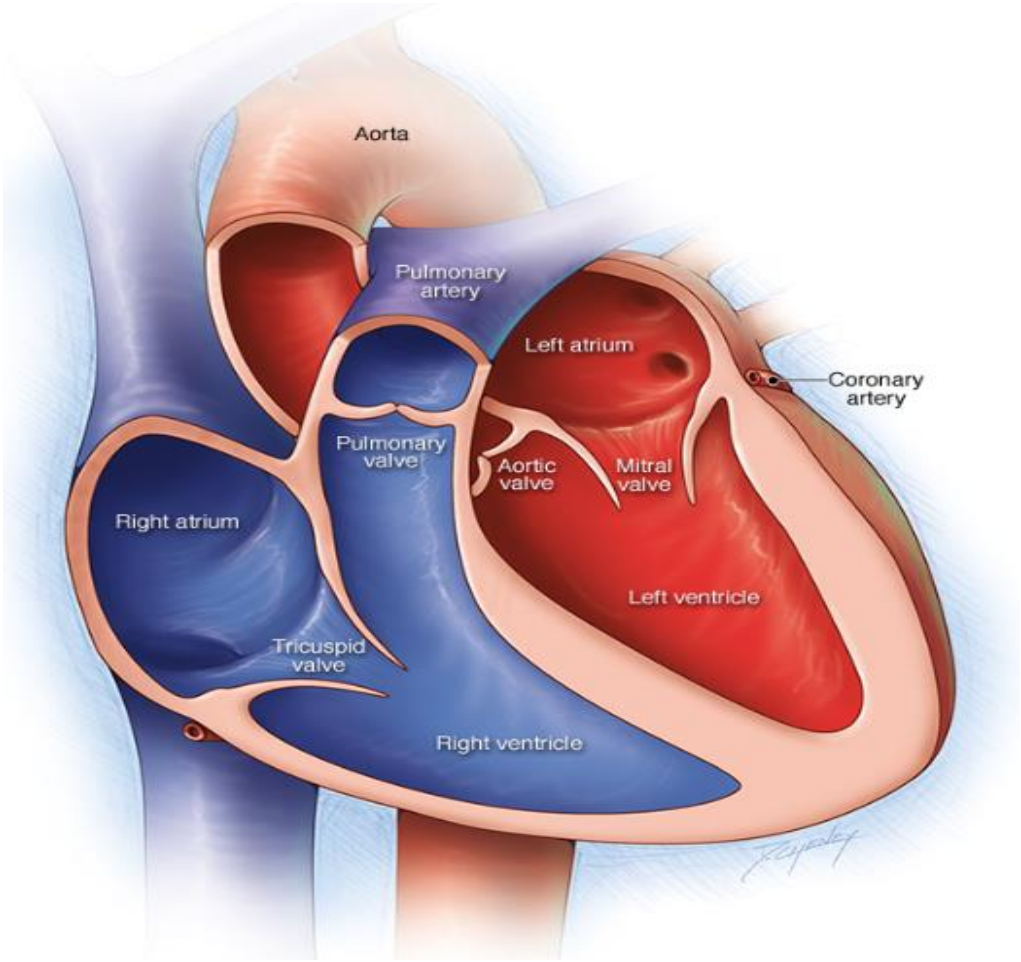

Figure 1. **Schematic of the Heart**. The chambers of the heart are shown, as well as the valves in which blood travels through to enter a new chamber, get oxygenated in the lungs and provide oxygen to the rest of the body (Mayo Foundation for Medical Education and Research, 2015).

The heart wall is called the pericardium and consists of 3 layers which include the epicardium, myocardium and endocardium. The epicardium is the outermost layer of the pericardium and has a purpose of encasing and protecting the heart. The epicardium allows for strong structural support composed of three membranous layers that encapsulate the heart. The first and outermost layer is called the fibrous pericardium and ensures stability of the heart when a person is running or jumping using support from the sternum and diaphragm. The middle layer is used to produce serous fluid to decrease friction against other structures in the body as the heart pumps. Lastly, the visceral pericardium is another serous producing tissue that is the inner most layer of the epicardium (Standring, 2008). Together, these layers fuse to form a space around the heart called the pericardial cavity. The myocardium is the actual heart muscle that is arranged in indistinct bundles that attach to heavy fibrous connective tissue that acts as the skeleton of the heart. The fibrous skeleton of the heart helps separate the muscles of the atria from the ventricles (Rosse, 1997). Lastly the endocardium is the innermost layer of the heart and is in contact with lumen of the heart and with the blood that enters the chambers (Milgrom-Hoffman et al., 2011).

1.2.2 Measuring Heart Function

The heart pumps approximately 5 liters of blood per minute at rest which can increase with an increase in exertion to about 21 liters and up to 35 liters depending on the fitness levels of an individual (Boron, 2005). It is advantageous to be able to measure the function of the heart by determining cardiac output. Other measurements include left ventricular end-diastolic

volume, left ventricular end-systolic volume, stroke volume and systolic ejection time. These measurements are typically used for research on left ventricular function and can provide an assessment of overall heart function. Diastolic contraction is the relaxation of the heart muscle which allows for the filling of the blood while systolic contraction is the contraction of the heart muscle which allows for the perfusion of blood to the rest of the body. During these contractions different measurements are acquired such as left ventricular end-systolic volume (ESV) which is the volume of blood in a ventricle at the end of systole. In contrast, left ventricular end-diastolic volume is the measurement of blood in the left ventricle at the end of diastole. Stroke volume (SV) is the volume of blood pumped from the left ventricle of the heart per beat. Lastly, systolic ejection time is the amount of time the ventricles spend in systole per minute (Cleland et al., 2011).

1.2.3 Myocardium Structure

Each muscle cell contains myofibrils that have repeating units called sarcomeres that consist of many smaller convoluted filaments called myofilaments. There are two types of myofilaments, myosin (thick filaments) and actin (thin filaments). Thin filaments consist of actin, tropomyosin, and troponin. Thick filaments in the myocardium are made up of polymerized myosin II proteins, each of these proteins having a total molecular weight of approximately 500 kD (Taylor, 1993). In cardiac muscle, sarcomeres are highly organized which give the tissue a characteristic of being striated, similar to skeletal muscle (Boron & Boulpaep, 2005).

Myosin II consists of a dimer of two heavy chains and two light chains associated with each heavy chain. Each myosin heavy chain weighs approximately 220 kD and contains a globular head domain which makes up the N-terminal domain and a C-terminal coiled-coil domain referred to as the tail. The tail allows dimerization and filament formation and contains a hinge which connects the tail to the head domain (Taylor, 1993). The globular N-terminal domain (S1 region) has a molecular weight of approximately 95 kD and contains the actin binding site and active site where ATP is hydrolyzed. S1 can be broken into three regions, a 25 kD NH_2-terminal region, a 50 kD central region and a 20 kD C-terminal region (Taylor, 1993). The essential and regulatory light chains (20 kD) bind to the light chain binding domain and can modulate ATPase activity in some myosins (Boron & Boulpaep, 2005).

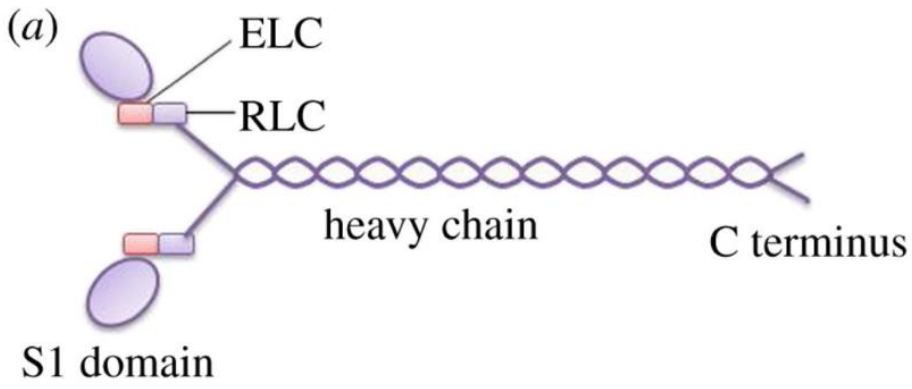

Figure 2. **Diagram Demonstrating the Different Regions of Myosin II**. The Myosin II is a component of myofibrils in skeletal, smooth and cardiac tissue. Lastly, the binding capabilities of this myosin allows for sliding filament theory capabilities (Chi, 2014).

Thin filaments are approximately 5 to 8 nm in diameter where they project from a dense disk known as the Z-disk which is perpendicular to the axis of the muscle fiber. The Z-disks

tether thin filaments of a single myofibril together and each myofibril to a neighboring myofibril. Thick filaments, however, are approximately 10 nm in diameter and they lie between thin filaments. Thick and thin filaments interdigitate resulting in the striated appearance. The light bands are thin filaments that do not overlap with thick filaments and are called I bands. The Z-disk can be seen as a dark perpendicular filament at the center of the isotropic band (I-bands). Additionally, the dark bands are the myosin filaments that overlap with the thin filaments to generate the anisotropic bands (A-bands) (Boron, 2005). Unlike the Z-disk being perpendicular and in the center of the I-band, the A-band has a less dense center which is identified as the H-zone. Titin, the largest of the cytoskeletal proteins in the muscular structure, traverses from the z-disk to the bare zone of myosin, region in the center of the thick filament that contains no crossbridges, where it is rigidly bound. Additionally, titin is responsible for regulating the passive elasticity of the sarcomere and stabilizing the A-band to the center of the sarcomere (Bagshaw, 1993).

1.2.4 Sliding Filament Theory

The sliding filament theory shows that A-bands, which contain thick filaments, do not change length during muscle contraction. In contrast to A-bands, I-bands diminish during contraction because the overlap between the filaments increases as the sarcomere shortens. H.E. Huxley and Hanson demonstrated in 1954, that when isolated myofibrils were induced to contract by adding ATP, the I-band and H-zone shortened in unison (Huxley, 1954). Electron microscopy has demonstrated connections between the thick and thin filaments called

crossbridges. When examining the thick and thin filaments in a relaxed state, the crossbridges were not distinct but were found to originate from the thick filaments (Bagshaw, 1993). The actin filaments are tethered by Z-discs and during contraction the sarcomere shortening occurs by bringing the Z-discs closer together (Figure 3). The sliding filament theory states that myosin molecules drive the sliding of actin past myosin generating muscle tension and shortening (Krans, 2010).

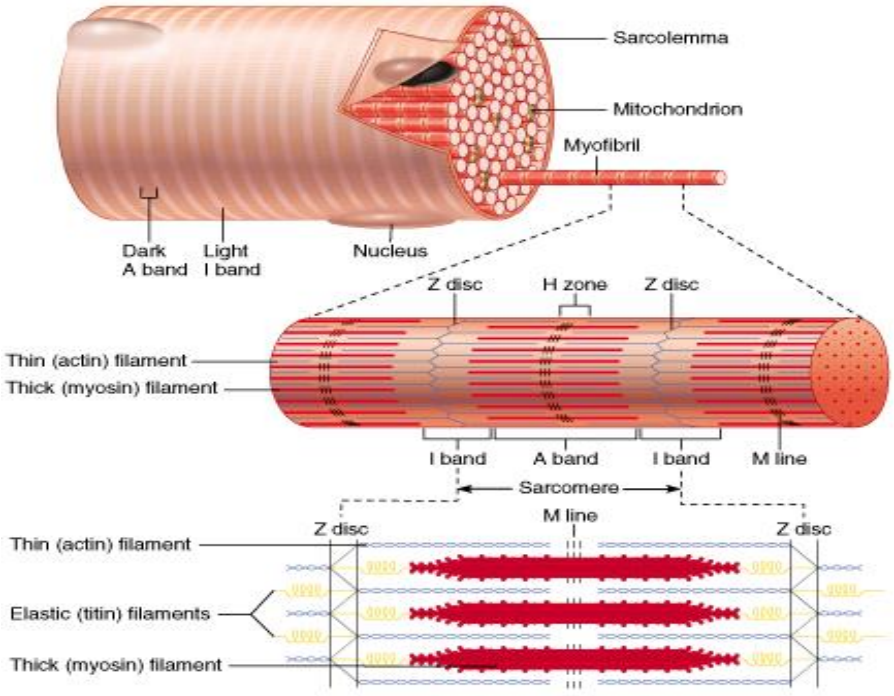

Figure 3. **Diagram of Striated muscle**. The anatomy of a sarcomere is composed of myofilaments that are found within myofibrils. The thick filaments (myosin) and thin filaments (actin) overlap which is important for the sliding filament theory (Cumming, 2001).

1.2.5 Actin/Myosin Interaction

At the molecular level, actin and myosin interact when the calcium released into the cytoplasm of the cell binds to troponin C, a regulatory protein component of the troponin complex associated with the actin molecule. The calcium bound to troponin C causes the troponin complex to shift the position of tropomyosin which exposes the myosin binding site on actin and allows myosin to interact with actin. The myosin head is predominantly in its "cocked" formation and creates a cross-bridge with the actin. To create a contraction, the energy for ATP hydrolysis is released causing the myosin power stroke. The power stroke is characterized by an approximately 45 degree angle change of the cross bridge resulting in a displacement of the actin filament about 11 nm toward the M-line. The crossbridges cycle between actin attached and detached states during the myosin ATPase cycle and each time a myosin head goes through an ATPase cycle it displaces the actin filament which causes muscle shortening (Huxley, 1954).

ATP binding to myosin dramatically reduces its affinity for actin and causes dissociation of the actomyosin complex (Raymond, 1996). The hydrolysis of ATP into ADP and P_i is rapid and occurs while myosin is detached from actin. The release of products (ADP and P_i) from myosin is catalyzed by the interaction between actin and myosin. With both ADP and P_i in the active site, myosin has a low affinity for actin. The affinity of myosin for actin increases when P_i is released. In the presence of ADP and without a nucleotide bound, the affinity of myosin for actin is high. Overall, the nature of the bound nucleotide will change the actin affinity, and result in what is referred to as the weakly and strongly bound states that are important for understanding sliding filament theory (Bagshaw, 1993).

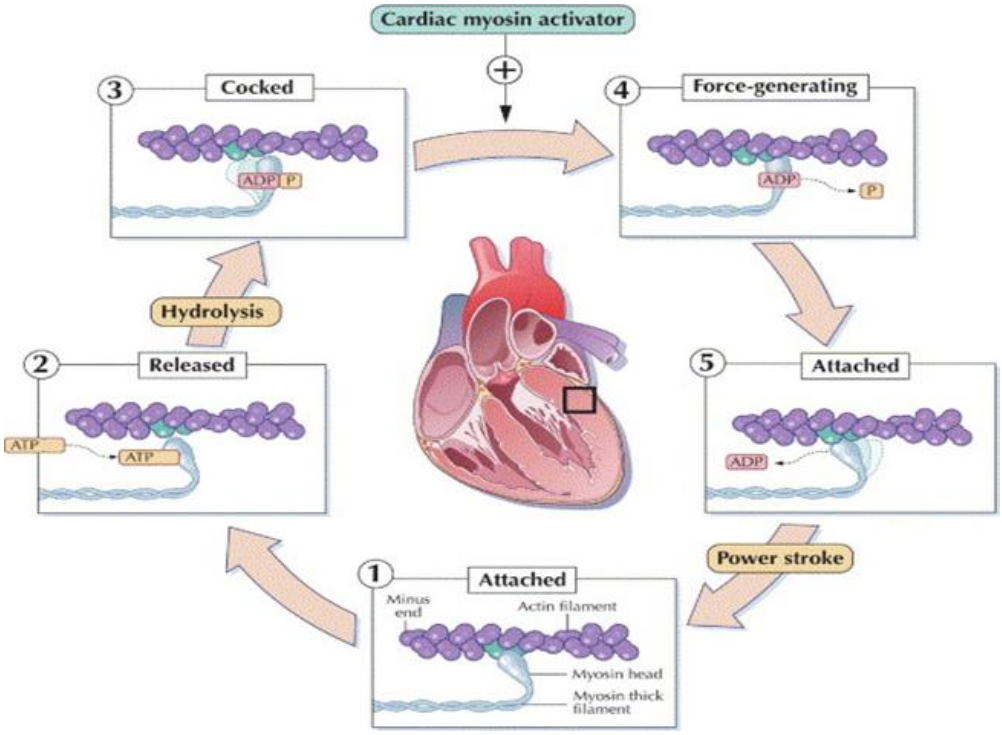

Figure 4. **ATPase Cycle of Cardiac Myosin**. This illustration presents the ATP hydrolyzes to ADP + P_i. The force production occurs during the actin activated product release steps. The diagram does not depict the influx of calcium into the cytoplasm and the movement of the tropomyosin in order to expose the attachment site on actin filament (Boron & Boulpaep, 2005).

The ATPase cycle can be divided into actin attached and actin detached states. The fraction of the ATPase cycle that myosin is bound to actin, divided by the total time required to complete an ATPase cycle is known as the duty ratio (Bloemink, 2011). The duty ratio is an important determinant of the number of myosin cross bridges that are generating force in a muscle fiber. Therefore, anything that changes the duty ratio can change the total force production generated by the myosin molecules in muscle.

$$Duty\ Ratio = \frac{Actin\ and\ Myosin\ Attachment\ Time}{Total\ Time\ to\ hydrolize\ ATP}$$

The rate limiting step for the ATPase cycle is the time it takes for the P_i to be released from myosin associated with the power stroke. The duty ratio can be changed by increasing ATPase cycle time or creating a longer attachment time. In a muscle fiber, this translates to an increase in the number of myosin force generators attached to actin at any given time (De La Cruz, 2004). For example, if we have a 10% duty ratio and 100 actin-myosin cross bridges in a muscle sarcomere, it will result in 10 out of the 100 cardiac myosin motors in the force generating state at any given time. If we increase the duty ratio to 20% and continue with 100 cardiac myosin motors available, we will have 20 out of the 100 cardiac myosin motors in the force generating state at any given time. Cardiac muscle myosin has a low duty ratio (≈0.05), therefore the actin and myosin attachment time is a small fraction of the ATPase cycle. This allows many myosin heads to work together in a muscle fiber without interference (Bloemink, 2011).

1.3 Impact of Heart Disease on Heart Function

1.3.1 Genetic Causes and Molecular Defects

As previously described, there are three major types of cardiomyopathies which include hypertrophic cardiomyopathy (HCM), dilated cardiomyopathy (DCM), and arrhythmogenic right ventricular cardiomyopathy (ARVC). The diversity of the cardiomyopathies results from genetic, allelic, epigenetic, and environmental heterogeneity (Schwartz et al., 2011). Heart disease affects multiple facets of cardiac function not only at the whole organ level but at the molecular level as well. For hypertrophic cardiomyopathies, analysis *in vitro* and in mouse models show

increased contractility of mutant myofilaments, changes in myosin kinetics, increases in calcium sensitivity of the thin filament, and changes in cardiac myosin binding protein C (cMYBP-C) mediated regulation (Schwartz et al., 2011). Increased sarcoplasmic calcium concentration during diastole is a catalyst for arrhythmias in mouse models. Mutations affecting thin filament regulatory proteins (tropomyosin, troponin T and troponin I) often increase calcium sensitivity by increasing the affinity of troponin C for calcium. Mutations can also alter cMYBP-C and myosin that can result in an increase in actin/myosin cross bridges. Troponin is the main calcium buffer in the sarcoplasm. Therefore, the increased calcium affinity should elevate calcium levels during diastole (Schwartz et al., 2011) and increases in calcium sensitivity were shown to increase peak force (Kataoka et al., 2007). The alterations to thin filament regulatory proteins may change the energy demands of the heart due to changes in the myosin ATPase. This is especially important because the cross bridge cycle accounts for approximately 70% of the energy consumption of the cardiomyocyte (Schwartz et al., 2011). Alterations in myosin ATPase can severely impact the energetic demands of the heart.

Dilated cardiomyopathies are characterized by left ventricle dilation, systolic dysfunction, cardiomyocyte death, and myocardial fibrosis. More than 40 genes linked to dilated cardiomyopathies have been identified which target components of a wide variety of pathways. Dilated differs from hypertrophic cardiomyopathy in that the affected genes encode for a wide variety of cellular components such as the nuclear envelope, contractile apparatus, the Z-discs, costamere, gene transcription, and calcium handling. The mutations found in the β-myosin heavy chain depress motor function while mutations in genes for thin filament regulatory proteins reduce calcium sensitivity which reduces ability to produce force.

Mutations in genes found to target the Z-disks can alter the structural boundary at each sarcomere. The heterogeneous nature of the mutations producing all of the different types of cardiomyopathies causes changes in cardiomyocyte structure and function. Though the identity of the cardiomyopathy is determined by different mutations, all lead to varying degrees of organelle and protein degradation resulting in heart failure (Schwartz et al., 2011).

Arrhythmogenic right ventricular cardiomyopathy is characterized by a fibrofatty replacement of myocardium. This characteristic has been found to mainly affect both ventricles resulting in the clinically witnessed, ventricular arrhythmias. Mutations in five genes that encode for desmosomal proteins have been found to contribute to ARVC by compromising cell-to-cell adhesion at intercalated disks resulting in the inability of myocytes to coordinate mechanical forces during the cardiac cycle. For example, reduced Wnt signaling, can be caused by mutant desmosomal proteins in progenitor cells, such as primitive right ventricular precursor cells, which makes them more susceptible of transforming into adipocytes (Schwartz et al., 2011). By targeting mutations with pharmaceutical interventions, mutations such as, reduction in Wnt signaling or elimination of the ineffectiveness of cell-to-cell adhesion, might be circumvented resulting in a correction or decrease in fibrofatty replacement of myocardium.

1.3.2 Clinical Effects

Most of the patients diagnosed with heart failure have failure in the left and right ventricles because those are the pumps that move blood to the pulmonary or systemic system, respectively. In patients with left ventricular failure, there is shortness of breath, blood in

sputum and chest pain. Upon examination, respiration and heart rate is elevated along with the possibility of weak pulses in patients suffering from severe left ventricular failure (McPhee, 1997). As previously stated, systolic contraction is diminished which leads to lower stroke volume. During systolic contraction, the atria and ventricles are contracted to move blood to the next location. In contrast, diastolic function is the relaxation of the atria and ventricles which allows them to fill with blood. To maintain cardiac output there is an increase in the return of blood to the heart, which leads to increased contraction of sarcomeres. The second compensatory mechanisms of the heart in failure is an increased release of catecholamines which increases heart rate. The third compensatory mechanism in heart failure is hypertrophy of the cardiac muscle and ventricular volume increase (National Institute of Health, 2011). These mechanisms are not long-term corrections and eventually lead to ultimate failure of the heart.

Symptoms of right ventricular failure include shortness of breath, pedal edema and abdominal pain. However, upon physical examination the findings are the same as those found in left ventricular failure. The most common cause of right ventricular failure is left ventricular failure, therefore the symptoms of left ventricular are often present. Additionally, there may be an elevated jugular venous pressure when observing the neck which is a good estimate of right atrial or central venous pressure. Both diastolic and systolic dysfunction can be caused by unnecessary loads placed on the ventricle or primary loss of myocyte contractility. Patients with right ventricular failure may also have a third heart sound heard at the sternal border (National Institute of Health, 2011). This third heart sound is called a protodiastolic gallop

which is the earliest cardiac physical finding of patients with significant heart failure (Dumitru, 2015).

In conclusion, heart failure is hard to diagnose if the patient does not have severe heart failure due to a lack of symptoms in the early stages. For example, stroke volume is not diminished at rest in patients with moderate heart failure however those with severe heart failure experience a decrease in pulse pressure and discoloration of the skin which is a sign of a decrease in stroke volume. Due to having different levels of heart failure, the American College of Cardiology collaborated with the American Heart Association to develop a guide to categorizing the stages of heart failure (Figure 5). This chart of stages is the first that incorporates risk factors due to patient history (Dumitru, 2015).

level	Description	Examples	Notes
A	At high risk for heart failure but without structural heart disease or symptoms of heart failure	Patients with coronary artery disease, hypertension, or diabetes mellitus without impaired LV function, hypertrophy, or geometric chamber distortion	▪ Patients with predisposing risk factors for developing heart failure ▪ Corresponds with patients with NYHA class I heart failure
B	Structural heart disease but without signs/symptoms of heart failure	Patients who are asymptomatic but who have LVH and/or impaired LV function	
C	Structural heart disease with current or past symptoms of heart failure	Patients with known structural heart disease and shortness of breath and fatigue, reduced exercise tolerance	▪ The majority of patients with heart failure are in this stage ▪ Corresponds with patients with NYHA class II and III heart failure
D	Refractory heart failure requiring specialized interventions	Patients who have marked symptoms at rest despite maximal medical therapy	▪ Patients in this stage may be eligible to receive mechanical circulatory support, receive continuous inotropic infusions, undergo procedures to facilitate fluid removal, or undergo heart transplantation or other procedures ▪ Corresponds with patients with NYHA class IV heart failure

Figure 5. **Stages of Heart Failure**. This chart is the ACC/AHA Stages of Heart Failure Development developed by the American College of Cardiology in collaboration with the American Heart Association. The chart not only identifies the development and progression of heart failure, but also recognizes risk factors for development of heart failure (Dumitru, 2015).

1.4 Heart Failure Interventions

1.4.1 Treatments

There is currently no cure for heart failure, however there are treatments that help manage the condition and improve quality of life for the patient (Mann, 2011). Patients with heart failure are typically put on inotropic agents such as β-blockers and calcium-channel blockers along with blood thinners (i.e. Heparin) and/or antidiuretics. There are two types of inotropic agents, positive and negative inotropes. Negative inotropes include beta-blockers, calcium-channel blockers and antiarrhythmic medicines, which all slow heart rate and weaken contraction by decreasing the amount of calcium released from the sarcoplasmic reticulum. Positive inotropic agents increase the force of each heartbeat and negative inotropic agents weaken the force of each beat. The goal behind using positive inotropes is to increase the amount of blood pumped out of the heart without changing heart rate. For example, digoxin increases calcium concentrations in cardiac cells to increase contractility by altering the sodium/potassium ATPase pump, which ultimately promotes the retention of calcium within the cell. An increase in calcium results in increased contractility of the heart (Texas Heart Institute, 2015). There are many other drugs that are administered which are aimed at sodium retention, arterial and venous constriction, neuroendocrine activation, increased heart rate, cardiac dissynchrony and arrhythmias (Cleland et al., 2011).

Though these medications can, in some cases, manage heart failure, they also can fail to alleviate symptoms or improve quality of life. Additionally, morbidity and mortality rates remain high for these patients. Though positive inotropic agents increase force and velocity of

contractility, they also shorten systolic contraction (Cleland et al., 2011). These drugs have the capabilities of creating negative long-term effects. For example, prolonged use of β-agonists could result in an increased sensitivity to calcium within the muscle. More specificially, β-agonists bind to β-adrenergic receptors which enhances the sympathetic response. β-adrenergic receptors are coupled to G-proteins which activate adenylyl cyclase and produce cyclic AMP (cAMP). The C-AMP then stimulates cAMP dependent protein kinase which phosphorylates the calcium channels and allows an influx of calcium which can increase the contractile force. Prolonged use of β-agonists has proven to increase calcium sensitivity and influx in cardiac muscle (Reiken, 2003). Therefore, prolonged use of β-agonists could cause a disruption in relaxation rates of the heart (Mant, 2011).

1.5 Omecamtiv Mecarbil

1.5.1 Background

To establish a drug that enhances contraction without altering calcium levels, drugs that directly target cardiac myosin were examined. Omecamtiv Mecarbil (OM) is a promising drug proposed to increase contractile force. OM is a small molecule drug that specifically targets cardiac myosin and is known to enhance force generation and improve energy utilization in cardiac muscle. What makes OM unique is it targets only cardiac myosin so it does not affect contractility of the myosin motors in other tissues within the body (Meijs, 2012). Furthermore, OM binds to a narrow cleft which separates the 50-K domain from the N-terminal 25-K domain (Figure 4) (Winkelmann, 2015). The goal of this drug is to increase the systolic ejection time

without changing diastolic time. Initial studies were done on animals while more recently, studies have been done in clinical settings while patients were on β-blockers.

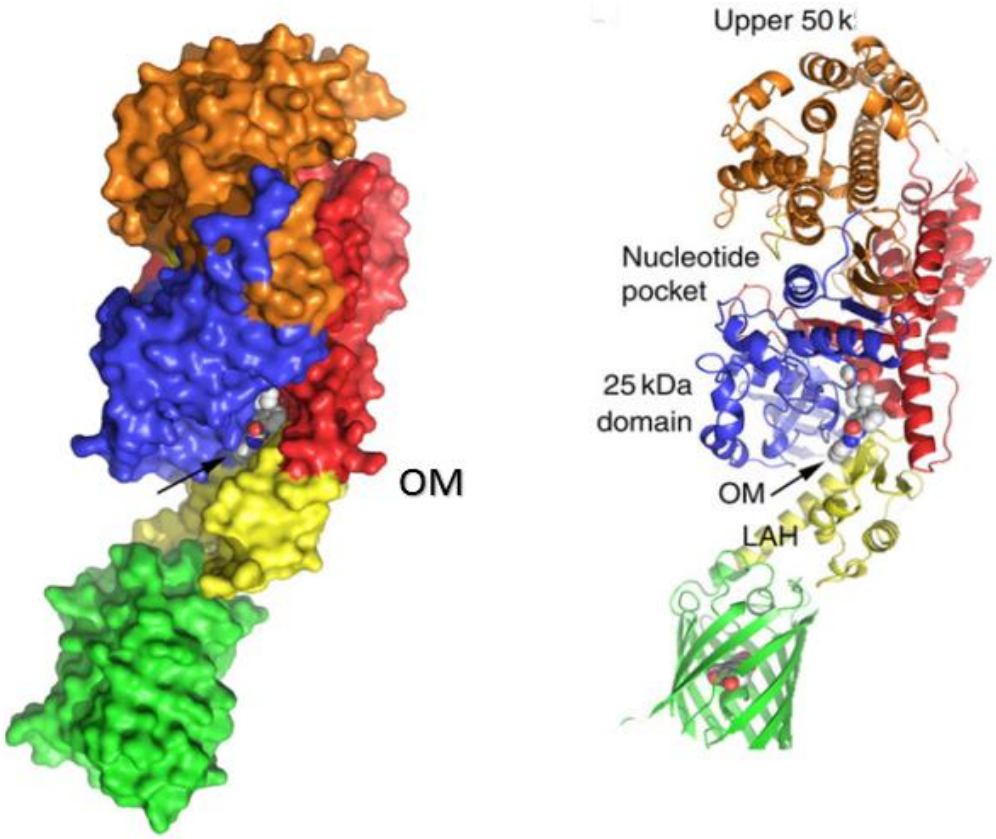

Figure 6. **Interaction of Omecamtiv Mecarbil with Human Cardiac Myosin**. This cartoon portrays the binding site for Omecamtiv Mecarbil separating the 50-K domain and N-terminal 25-K domain (Winkelmann, 2015).

1.5.2 Effects on Actin and Myosin

Malik et al., showed that the activator drug, Omecamtiv Mecarbil, binds directly to cardiac muscle myosin and acts as an allosteric effecter to stimulate motor activity and enhance cardiac functionality without altering calcium sensitivity (Malik et al., 2011). OM binds to the S-1 domain of the cardiac myosin by binding to the base of the lever arm where the relay helix

and the converter domain come together (Winkelmann et al., 2015). Recent studies demonstrate that OM increases the equilibrium constant in the hydrolysis of ATP to ADP and Pi with an unchanged ADP dissociation from actomyosin (Liu et al., 2015). This kinetic change shows an increase in myosin heads competence to produce force. Additionally, Winkelman et al. (2015) concluded, that OM binding between the N-terminal 25-K domain and the 50-K domain acts to stabilize the interactions within the coupling region, with the motor and lever arm region. These allosteric changes were shown to induce changes in locations distant from the cleft in which OM binds. Liu et al. was also able to support that the drug binding shifts the hydrolysis equilibrium constant and enhances phosphate release. They found that the hydrolysis equilibrium constant increased from 2.4 in the absence of OM to 6 in the presence of OM showing a shift further towards hydrolysis or product formation in the presence of OM (Liu, 2015). Previous results suggest mechanical tuning of β-cardiac myosin may be critical for altering force velocity relationship in cardiac muscle (Greenberg et al., 2009).

1.5.3 Animal Studies

Before analyzing OM at the whole organ level, investigators used animal models to analyze the specific actions of OM within myofibrils. Mamidi et al. took myofibrils from frozen rat left ventricles that contained no myosin binding protein-C, which is known to decrease in heart failure, and examined muscle mechanics in the presence of OM. The knockout of cMyBP-C was to stimulate hypertrophic cardiomyopathy with reduced cMyBP-C levels in cardiac muscle. However, when this myocardium was incubated in OM, the crossbridge contractile

velocity was decreased. To gain additional information, Mamidi et al. (2015), investigated the function of OM at different levels of calcium concentrations to determine the impact of calcium sensitivity. They found that at lower calcium concentrations, OM increased force generation while it had little impact at higher calcium concentrations. They were able to conclude that OM increased myofilament calcium sensitivity which supports the hypothesis that OM would enhance recruitment of force generating myosin heads (Mamidi, 2015).

Porcine ventricular heavy meromyosin (HMM) which is a β-cardiac myosin isoform, was used in a study to investigate the effect of OM on the ATPase cycle. As previously mentioned, Liu et al. (2015), were able to demonstrate that OM shifts the equilibrium of the hydrolysis step to favor the M.ADP.P_i state (Liu, 2015). Liu et al., demonstrated a decrease in *in vitro* sliding velocity and explained these results by hypothesizing that the increase in strongly bound myosin heads results in increased force but decreased velocity. They also found that there was no change in ADP dissociation hence suggested that the slower velocity is caused by increased load sensitivity. According to their findings, OM should not be considered a myosin ATPase activator, but an allosteric effector that leads to an increase in force generation in the heart (Liu, 2015).

In 2015, Nagy et al., used skinned rat cardiomyocytes and diaphragm muscle fibers to investigate the calcium sensitizing effects from the administration of OM. The goal of the study was to determine how OM effects the activation and relaxation cycles within muscle and the tissue selectivity of OM. The purpose of targeting diaphragm muscle was to see if OM could also change the function of diaphragm muscle in a manner similar to cardiac muscle. The investigators found that OM altered the activation and relaxation in cardiomyocytes as previous

studies have shown, but also found that OM had a calcium sensitizing effect on the diaphragm muscle as well. In this study, OM increased calcium sensitivity at a concentration of 0.1 μM and higher. Nagy et al. (2015) linked the slow kinetics seen *in vitro* to no change in left ventricular pressure. The researchers suggested that differences in OM concentration between maximal and submaximal activations may contribute to these findings. Furthermore, a substantial increase in calcium sensitivity was found in diastole and increased the passive force of these cardiomyocytes in the presence of OM. The drug also caused a prolonged relaxation in the myocytes following calcium dissociation from thin filaments. In conclusion, they found that OM activation was similar to that of calcium sensitizing positive inotropic agents and that it may also cause calcium sensitization in diaphragm fibers with slow intrinsic kinetics (Nagy, 2015).

1.5.4 Human Studies

The first human study was performed by Teerlink et al. (2011) to investigate whether OM caused any augmented human cardiac function. This study was a dose-escalating, cross-over study where 34 men were given six hour double blind intravenous infusion of OM or a placebo once a week for four weeks. Each sequence consisted of three ascending OM doses ranging from 0.005 to 1.0 mg/kg per hour with placebo infusion randomized into the sequence. Teerlink et al. (2011) proceeded to monitor vital signs, blood samples, electrocardiograms and echocardiograms before, during and after each infusion. The investigators found that OM had highly dose-dependent pharmacokinetic characteristics, patients tolerated up to 0.625 mg/kg per hour as determined by the onset of myocardial ischemia and excessive prolongation of

systolic ejection time. At this drug level, OM increased systolic ejection time with proportional augmentation of systolic function. Additionally, OM increased atrial contractile function, without producing functional changes in diastolic contraction. There were also no reported effects on blood serum chemistries, vital signs or ECGs (Teerlink, 2011).

Teerlink and Cleland et al. (2011) continued their investigation of OM with a phase 2 trial by performing a double-blind, placebo-controlled, crossover, dose-ranging study that provided patients with intravenous OM for 2, 24 and 72 hours in patients with stable heart failure and left ventricular systolic dysfunction. As in the first trial, the investigators obtained vital signs, echocardiograms, electrocardiographs and blood samples to test blood serum levels of OM. There were 45 patients that received 151 infusions of OM or placebo with analysis of seven concentration bin groups: placebo, 0 to ≤100, >100 to ≤200, >200 to ≤300, >300 to ≤400, >400 to ≤500, and >500 ng/mL. As a result, OM had dose-dependent (amount of time OM is bound/administered) and concentration-dependent (amount of OM bound) effects on cardiac function at plasma concentrations that are well tolerated by stable systolic heart failure patients. Systolic ejection time, stroke volume and fractional shortening increased in a concentration-dependent manner. Plasma concentrations of OM greater than 100 ng/mL increased systolic ejection time and fractional shortening as compared with placebo. Stroke volume increased by 5–10 mL at plasma concentrations higher than 200 ng/mL, reaching a plateau at concentrations greater than 400 ng/mL. Additionally, plasma concentrations higher than 300 ng/mL were associated with an increase in left ventricular ejection fraction and reductions in left ventricular end-systolic and end-diastolic volume were significant at 500

ng/mL. Plasma concentrations greater than 1200 ng/mL were not clinically tolerated in two of three patients who exceeded those levels (Cleland, 2011).

1.5.5 Future for Omcamtiv Mecarbil

Though there is some optimism in using OM as a myosin activator to combat heart failure in a safer fashion than inotropic agents, there is still a strong need to investigate the specific mechanisms of OM on cardiac myosin function. With a known binding site and knowledge about the effects of OM on the ATPase cycle, we still do not know the mechanism by which OM slows the sliding velocity. Investigation into the mechanisms behind the effects of OM as well as the dose dependence in human studies still needs to be completed. Experiments at the molecular level will need to be put into the context of *in vivo* function to accurately examine the mechanism of action in combating heart failure. Lastly, long-term human studies are needed to gain knowledge about the optimal OM dosage and the long-term side effects.

Chapter 2: Goals and Hypothesis

2.1 Hypothesis

Our hypothesis is that the drug, omecamtiv mecarbil (OM), enhances force generation of cardiac myosin by increasing the duty ratio. Our rationale is that, with a longer attached time, OM will lead to a higher duty ratio which will result in an enhancement in the number of force generating myosin motors in muscle. Therefore, we would not only see an increase in force generation in heart failure patients, but in normal patients as well. Such knowledge would demonstrate the mechanism of how OM enhances force generation in cardiac muscle. Previous results suggest that myosin is a good drug target for heart failure patients. In addition, by studying how OM impacts cardiac myosin from heart failure patients, we were eager to gain knowledge on how the drug may be utilized to increase force generation in heart failure patients.

Previous research has proven that OM will decrease velocity in the *in vitro* motility assay, however the mechanism for how this occurs is still unclear. We propose that the increase in actin affinity also comes with added strain caused by many cardiac myosin motors interacting with the same actin filament. More specifically, we suspect that not only are more myosin heads attached to the thin filaments, but a percentage of these attached heads are not force producing. If some of the myosin heads are producing force and others fail to do so, then there are myosin heads staying attached that create a drag force which could contribute to the decrease in sliding velocity.

2.2 Specific Aims

2.2.1 To examine the impact of OM on cardiac myosin motor performance

We first aimed to examine how OM impacts cardiac myosin performance. In the lab, we expressed myoblasts into cardiac myosin from a C2C12 expression system and examined cardiac myosin motor performance with and without OM using *in vitro* motility and ATPase Assays. Our hypothesis was that there would be an increase in force generating capacity of cardiac muscle myosin in the presence of OM by increasing duty ratio.

2.2.2 To determine the impact of the cardiac myosin activator drug (OM) on myosin isolated from heart failure patients

Our second aim was to examine the impact of the cardiac myosin activator drug (OM) on myosin isolated from heart failure patients. Many of the patients that have donated their cardiac tissue to the Biobank at the University of Kentucky did so after having an LVAD (left ventricular assistive device) implanted or a heart transplant. We planned to examine how OM alters cardiac muscle myosin from a recombinant expression system, which would be compared to the tissue isolated myosin. We hypothesize that OM will enhance motor performance of cardiac myosin isolated from heart failure patients similar to recombinant cardiac myosin.

Chapter 3: Methods

3.1 Introduction

We examined cardiac myosin purified from human heart failure patients. The tissue was donated from the University of Kentucky Biobank. We extracted and purified human full length β-cardiac myosin (M2B) from the tissue. Expression and purification of the recombinant cardiac myosin from a C_2C_{12} expression system was also performed. An N-terminal flag tag was inserted onto the M2B-S1 construct for purification. For *in* vitro motility assays, a C-terminal Avi tag was inserted to allow specific attachment to the motility surface. *In vitro* motility assays were performed to evaluate the actin sliding velocity generated by myosin while the ATPase activity was evaluated through performing ATPase assays.

3.2 In *Vitro* Motility Assay

3.2.1 History

Several *in vitro* motility assays have been developed to examine the movement of actin filaments generated by myosin motors. Either F-actin or myosin is anchored to a stationary surface while the movement of its counterpart is tracked to obtain a velocity of movement (Sivaramakrishnan, 2010). The actin filaments exhibit ATP-dependent movement over the myosin-coated surface while following winding paths without reversing their direction of movement by progressing from one myosin head to the next. The rate of movement depends

on the concentration of ATP. In the absence of ATP, filaments bind to the surface but will not move. As the concentration of ATP is increased, the velocity of the fluorescent actin increases until the asymptotic velocity at saturating ATP concentration is reached at approximately 100 µM ATP (Kron, 1986).

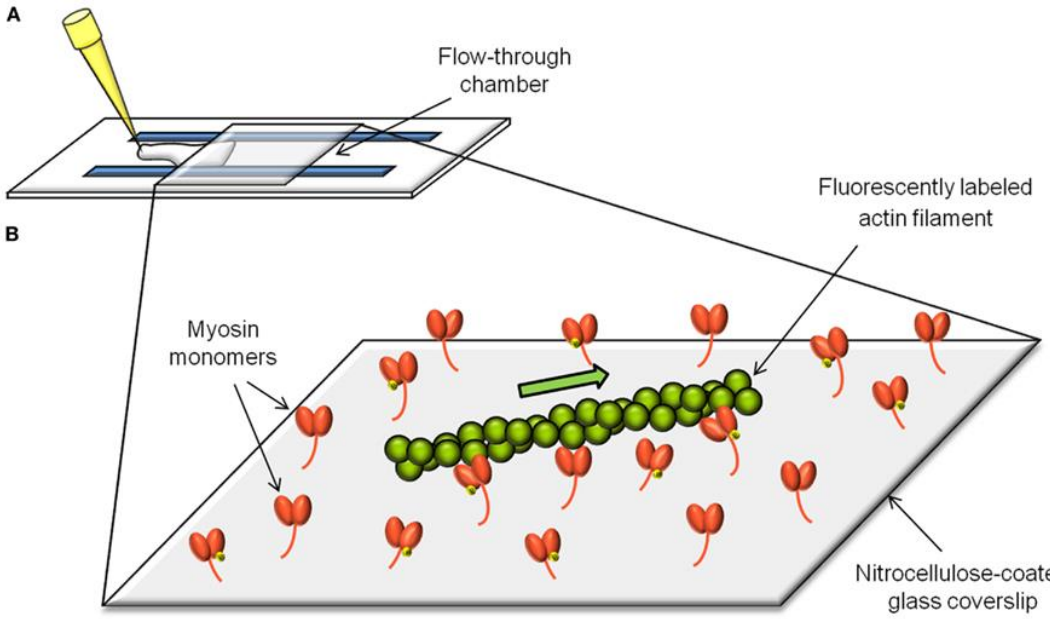

Figure 7. **Diagram of *In Vitro* Motility Assay**. This drawing shows a saturated concentration of myosin which is adhered to the nitrocellulose on the coverslip. Additionally, the presence of ATP interacts with fluorescently labeled actin filaments, propelling them across the surface of the slide (ELauzon, 2015).

The most important aspect to the *in vitro* motility assay is that it produces the ability to rapidly, quantitatively and repeatedly examine motor based movement from small samples of purified proteins (Kron, 1986). Low concentrations of motor proteins on the surface in the *in*

vitro motility assay enforces little load against which the myosin needs to work, suiting this assay to study motor function in the absence of load (Sivaramakrishnan, 2010). The assay allows for the addition of factors that may modify myosin or actin within the assay, and determine how these factors influence actin movement. The *in vitro* motility assay has become the standard assay and has been used to characterize the function of many myosins, including myosins I, V, VI, IX and X (Sivaramakrishnan, 2010).

3.2.2 *In Vitro* Motility Assay Technique

We examined velocities of the actin-myosin interactions by using the *in vitro* motility assays which utilizes fluorescence microscopy. The time-lapsed video microscopy was obtained using NIS-Elements Viewer 4.0 Software and velocities were analyzed with ImageJ software. To create the flow cell we coated a microscope cover slip with nitrocellulose and let it dry for ≈10 min. Once the flow cell is made we flowed through MOPS 20 buffer without DTT (30µl). Next, 15µl of streptavidin was added and incubated at room temperature for 3 min which allowed it to adhere to the nitrocellulose coverslip. Once again MOPS 20 buffer without DTT (30µl) was used to remove unbound streptavidin followed by an injection of 30µl of 1 mg/ml BSA incubated at room temperature for 1 min to block non-specific binding sites on the surface. A wash with MOPS without DTT (30µl) was the final wash prior to the application of myosin. Next, 15µl of M2B-S1 of different dilutions per assay was incubated at room temperature for 3 minutes to allow adhesion to the streptavidin-coated slide coverslip. We washed the flow cell with MOPS 20 buffer with DTT (30µl). 15µl of unlabeled shear actin was applied followed by

30µl of 2mM ATP. This step blocks the sites that are associated with dead myosin (dead-heads). At this time, a wash was used with MOPS 20 buffer with DTT (30µl) to precede the addition of 15µl fluorescently labeled ALEXA actin. The ALEXA actin was allowed to incubate at room temperature for 1 min to bind the myosin heads to the surface. Lastly, we added 15µl activation solution containing 0.14% Methylcellulose, 1 mg/mL BSA, and the ATP regeneration system (phosphoenolpyruvate carboxylase and pyruvate kinase). To prevent photobleaching, 0.5µl of GOC (glucose oxidase catalase) and glucose was used in MOPS 20 buffer with DTT. The activation buffer also contained 2mM ATP and either 0.1% DMSO or 10µM OM (in 0.1% DMSO) to assess the effects of OM. Once these steps were completed the slide was examined to measure the movement of actin filaments as a function of time using fluorescence video microscopy.

We measured the velocity for each actin filament and the average of ≈30-50 filaments was examined. These averages were plotted, with the velocities on the y-axis and the myosin dilutions on the x-axis. We also plotted the velocity vs actin filament length. The duty ratio was examined by fitting velocity vs actin filament length data to the established equation (Harris and Warshaw, 1993). The plots of velocity vs myosin density were fit to a hyperbolic function to determine the relative trend of the results.

3.3 ATPase Assay

3.3.1 History

Steady-state ATPase assays and stop flow kinetic measurements are used to determine the actomyosin ATPase kinetics (Sivaramakrishnan, 2010). The general pathway of the ATPase cycle that was presented earlier is fairly conserved among all of the myosin classes; however, the rates and equilibrium constants of each step different for each myosin class. Examination of the ATPase cycle allows determination of the lifetimes and relative populations of key biochemical intermediates, which directly correlate with the functional capacity of myosin at a cellular level (De La Cruz, 2009).

The most commonly performed ATPase assay involves a steady-state measurement of the maximum ATPase rate of a myosin and its apparent affinity for actin. In the steady-state ATPase assay, a known concentration of myosin is mixed with a series of increasing concentrations of actin filaments, in the presence of saturating levels of ATP (Sivaramakrishnan, 2010). The stop-flow apparatus measures absorbance of NADH per unit of time and the data are fit to a linear equation to obtain the slope. A control sample of actin without myosin was subtracted from the actomyosin sample. The ATPase assay is based on the conversion of phosphoenolpyruvate (PEP) to pyruvate by pyruvate kinase (PK) coupled to the conversion of pyruvate to lactate by lactate dehydrogenase (LDH). The later step requires NADH which is oxidized to NAD+ while NADH absorbs strongly at 340 nm but NAD+ does not. This enables the examination of NADH absorbance that can be monitored at 340 nm. The absorbance per unit

time can be converted into ATPase activity where 1 molecule of NADH oxidized to NAD+ corresponds to the production of 1 molecule of ADP produced by the motor ATPase.

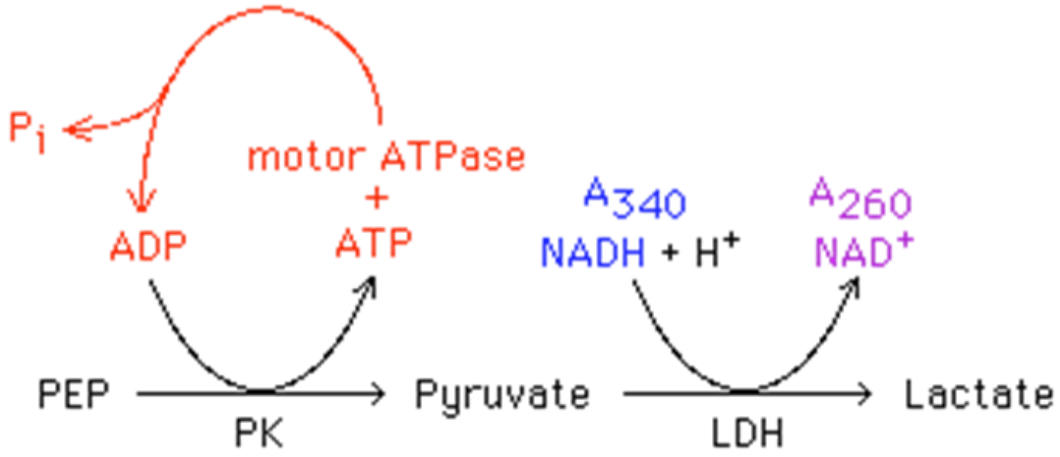

Figure 8. **Diagram NADH-Coupled Assay in ATPase Experiment**. This cartoon portrays the NADH-coupled assay for measuring myosin ATPase activity (Greene, 2011).

An ADP standard curve is used to convert absorbance units to ADP concentration. The ADP/sec is then divided by the concentration of myosin to determine the amount of product formation per unit of time per myosin head. By pairing this assay with the *in vitro* motility assay, we are able to examine the impact of OM on myosin function.

3.3.2 ATPase Assay Technique

ATPase assays were performed using multiple dilutions of actin with a constant concentration of myosin in the presence of OM or a DMSO control. The maximum ATPase rate (K_{cat}) and actin concentration at which the ATPase activity is ½ the maximum (K_{ATPase}) were

obtained by fitting the data to a hyperbolic function. We used a standard buffer of MOPS 20 with DTT (10mM MOPS, 20mM KCl, 1mM EGTA, 1mM $MgCl_2$, 1mM DTT) to perform the assay at 25^o C. In each dilution of actin, 0.1µM of myosin and 1mM ATP was added to the sample just before it was injected into the stop flow. The stop-flow measures absorbance of NADH per unit of time and we fit the data to a linear equation to obtain the slope. A control sample of actin without myosin was subtracted from the actomyosin sample. The standard curve was used to convert absorbance units to ADP concentration. The ADP/sec was next divided by the concentration of myosin to determine the amount of product formation per unit of time per myosin head. The data were plotted in Kaleidograph software to fit the data to a hyperbolic function to determine K_{cat} and K_{ATPase}. Lastly, t-tests were calculated in the tissue samples to determine the significance of differences in the DMSO and OM samples.

Chapter 4: Results

4.1 ATPase Assay OM vs DMSO

The ATPase assay was performed using M2B-S1 prepared from a C2C12 expression system. In each actin sample, 0.1µM of myosin and 1mM ATP was added prior to injecting the sample into the stop flow at 25^o C. Absorbance changes were documented at 340nm while actin concentrations varied from 5µM to 60µM. The results, with and without OM, were then compared with a scatter plot in the KaleidaGraph software. The graph shows a dramatic difference in the parameters determined in the presence of DMSO or OM. We determined that

the maximum ATPase activity was reduced approximately 6-fold in the presence of OM while the actin affinity was greatly enhanced in the presence of OM as indicated by the 16 fold decrease in the K_{ATPase} (Figure 9).

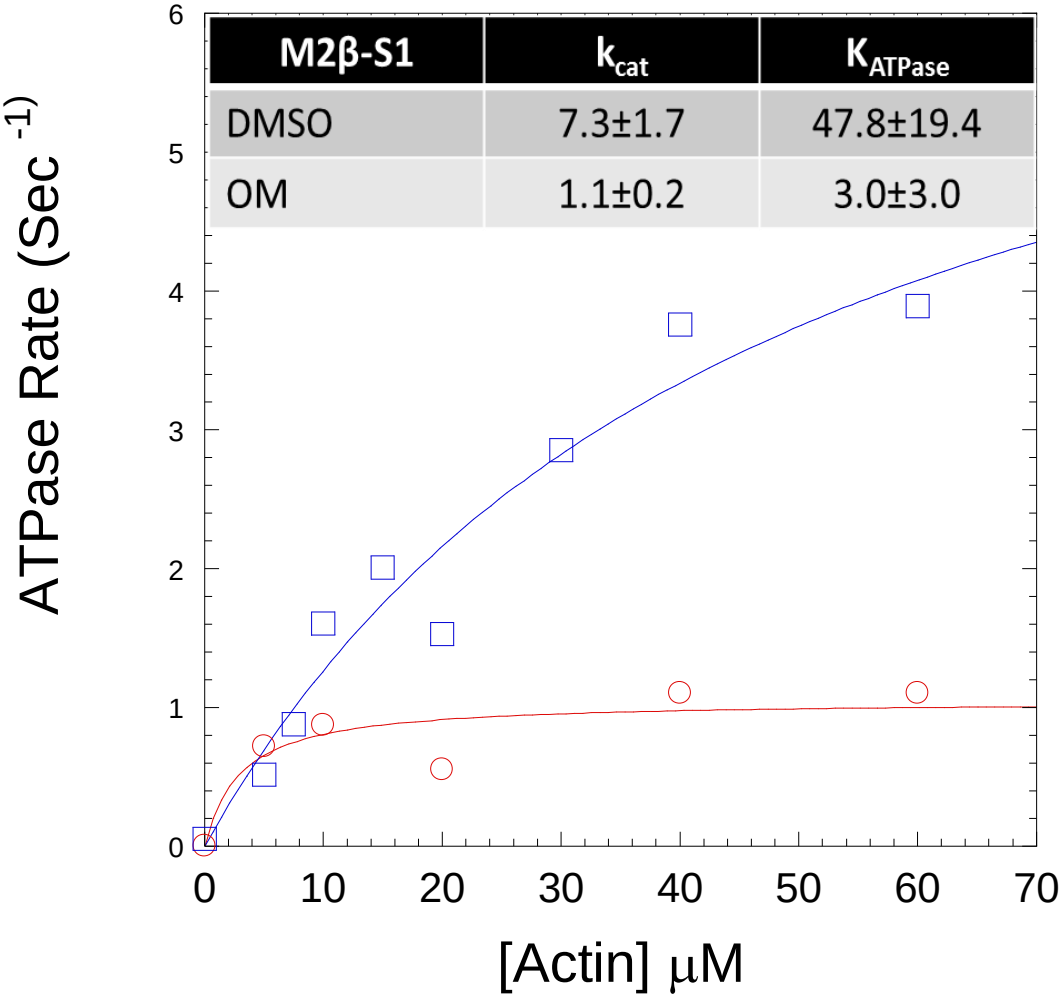

Figure 9. **Actin-activated ATPase Activity of M2B-S1 in the Presence and Absence of OM**. The ATPase activity is plotted as a function of actin concentration and fit to a hyperbola to determine the maximum ATPase activity (K_{cat}) and dependence on actin concentration (K_{ATPase}). The ATPase parameters are summarized in the table in the inset. k_{cat} was 7.3±1.7 for DMSO and 1.1±0.2 for OM while the K_{ATPase} for DMSO was 47.8±19.4 and k_{cat} 3.0±3.0 for OM.

4.2 *In Vitro* Motility Assay OM vs DMSO

The motility assay is performed by using a Nikon TE200 fluorescent microscope which allows for generating time lapsed videos using NIS-Elements Viewer 4.20 software. Once the videos are acquired, ImageJ software is used to examine the video one frame at a time which allows for the determination of tracks where the actin filament sliding occurred. ImageJ software is capable of calculating the distance traveled by the fluorescently labeled actin per frame according to the determined tracks. In the videos taken with DMSO added, there are longer tracks and faster movement of filaments therefore more frames are taken in a shorter amount of time (1 frame per second 3 minutes or 181 total frames). In contrast, videos taken after the addition of OM move at a much slower velocity. Hence, more time is needed between each frame to capture the slow movement making the video less frames but more time in order to produce long enough tracks to assess average velocity (1 frame per 15 seconds for 10 minutes or 41 total frames).

By looking at the same number of frames at the same intervals in Figure 10, the results show that tracks are longer for DMSO than for OM, which translates to a 100-fold difference in sliding velocity. More specifically, the two DMSO velocities that were analyzed in **(A)** were averaged at 1506.998 nm/sec (Red) and 1470.819 nm/sec (Yellow). The two averages acquired for the OM video **(B)** were 13.070 nm/sec (Red) and 11.428 nm/sec (yellow). Figures A and B highlight that in the same number of frames, the distance traveled by fluorescent actin filaments in the presence of OM is dramatically reduced compared to the absence of OM.

We examined the velocity of filament sliding in a large number of filaments to determine the distribution of velocities in the presence of OM or DMSO. By examining approximately 200 filament velocities for DMSO or OM and binning the sliding velocities into groups, we compared the distributions in a frequency plot (Figure 10, C and D). These graphs show the affect OM has on myosin function by demonstrating that the sliding velocity decreases from an average of 1343 nm/sec in the presence of DMSO to 13.1 nm/sec in the presence of OM. This 100 fold decrease in filament velocity in the presence of OM is much greater than the decrease examined in the ATPase assay.

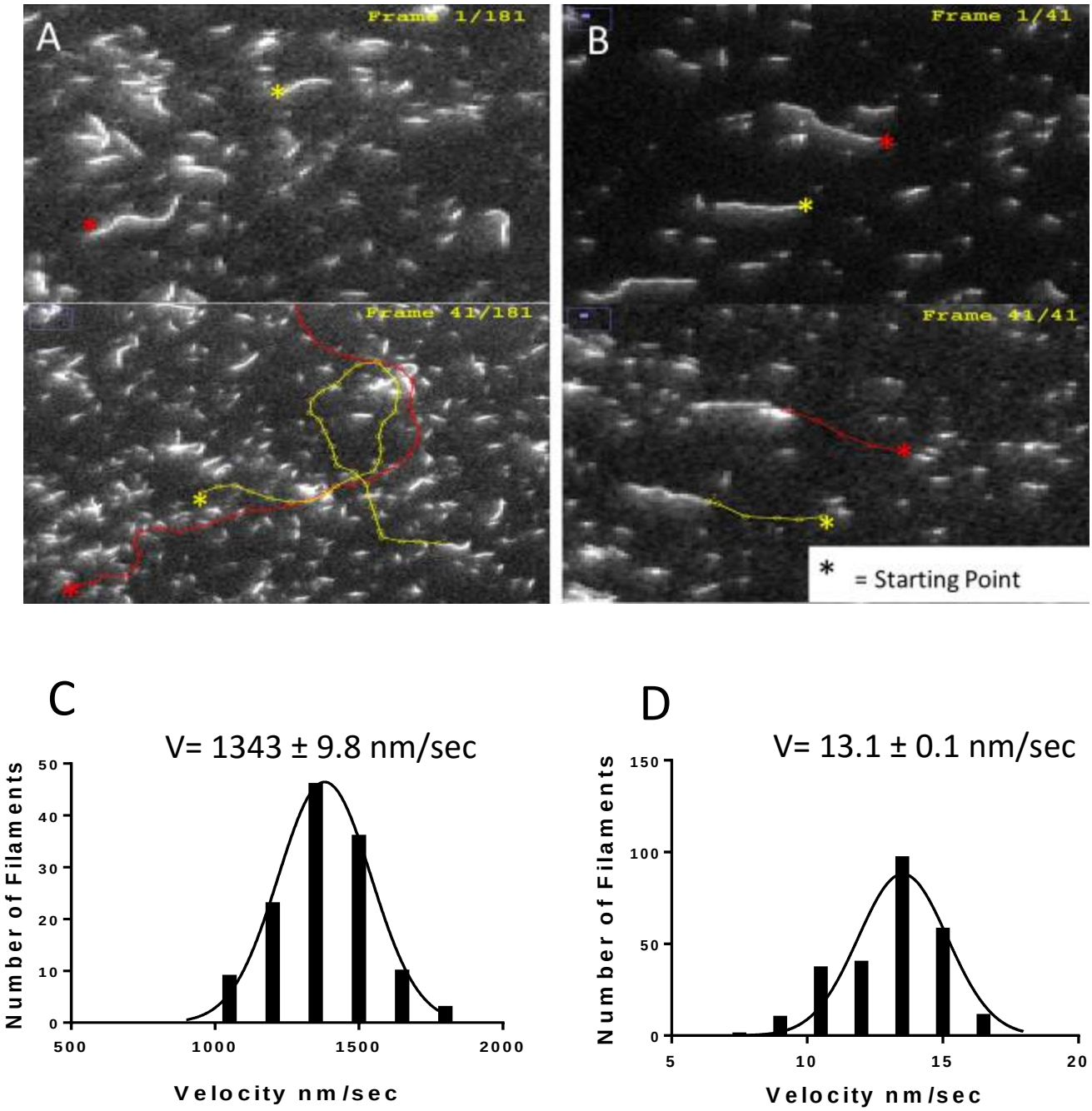

Figure 10. ***In vitro*** **motility assay in presence and absence of OM**. The time lapsed videos show the length of two tracks following the tail of a fluorescently labeled actin filament from frames 1 to 41. Average velocities were distributed to the amount of filaments moving within different velocity ranges **(A)** On the left represents the tracks and velocities created in DMSO, and **(B)** on the right, in the presence OM. **(C)** Velocities of filaments with DMSO were grouped by binning at an interval of 150 while **(D)** velocities of filaments in the presence of OM were binned at an interval of 1.5. The standard error was similar for both conditions (±7%). Average velocities and tracks were developed in ImageJ software after acquiring videos with NIS-Elements Viewer 4.20 software along with a Nikon TE200 fluorescents microscope.

4.3 M2B Density Dependence

The density dependence is performed to investigate the impact of changing the amount of M2B-S1 on the motility surface. This was done by examining the sliding velocity as a function of myosin density in the presence of (A) 0.1% DMSO or (B) 10% μM OM. In the presence of DMSO the velocity increases as a function of density until maximum velocity is achieved. In the presence of OM, we observed higher velocities at lower densities. The inverse dependence on density is interesting, since it is the opposite of that observed without OM. Our results support the model that the higher affinity for actin in the presence of OM causes more drag forces which are greater at higher myosin surface densities.

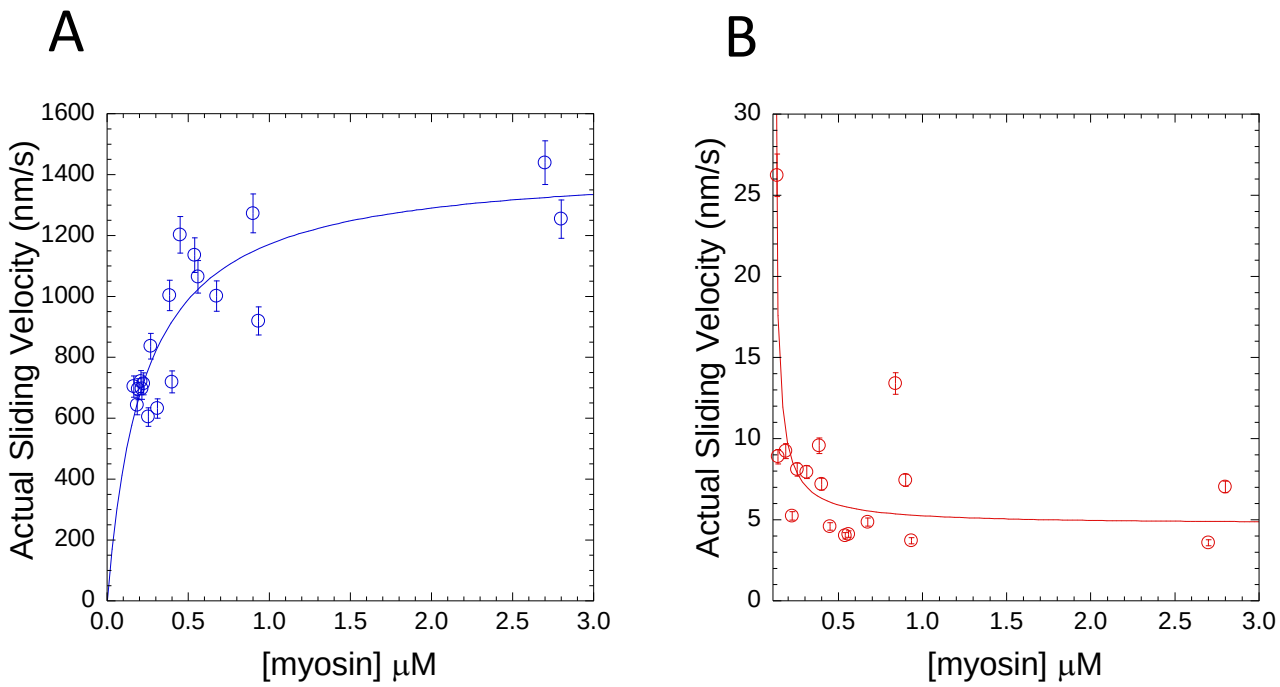

Figure 11. <u>Density Dependence of *In Vitro* Motility in the Presence and Absence of OM</u>. Different dilutions of myosin were applied to the motility surface. The videos were developed by NIS-Elements Viewer 4.20 software using fluorescent microscopy and analyzed using ImageJ software. Once the videos were analyzed the velocities of 30 filaments per density plotted using KaleidaGraph software. Sliding velocities were plotted as a function of myosin concentration to determine the density dependence. Chart **(A)** shows the density dependence chart with DMSO and chart **(B)** density dependence chart with OM.

4.4 Length Dependence

In actin filament length dependence evaluations, the density of the myosin on the surface is kept constant. Lengths were obtained through ImageJ software by manually measuring the lengths of 200 filaments that were tracked. In Figure 11, **(A)** and **(B)** velocity measurements were normalized by dividing each velocity by the average velocity. The normalization of the velocities allows a direct comparison of DMSO and OM. Our hypothesis is that longer filaments provide more surface area which results in greater velocities because more myosin heads are interacting per actin filament. In contrast, smaller filaments will provide less surface area for crossbridge formation which is proposed to reduce velocity.

The length vs velocity data is fit to an equation that takes into account the myosin density and the duty ratio. We fit the data to the following equation:

$$v = (1 - V_{max}) \times \{1 - (1 - f)^N\}$$

where f equals the crossbridge duty ratio and N equals the total number of crossbridges capable of interacting with actin. The term (V_{max}) refers to the efficiency of transmitting maximum velocity achieved at high density (Harris and Warshaw, 1993). After collecting length and velocity of sliding actin filaments, we observed no change in duty ratio with results of 0.041 ± 0.014 in the presence of DMSO and 0.049 ± 0.020 in the presence of OM at a myosin concentration of 1.3 µM. However, with a decrease in myosin concentration to 0.2 µM, we witnessed a 2-fold increase from 0.058 ± 0.047 in the presence of DMSO to 0.094 ± 0.013 in the presence of OM.

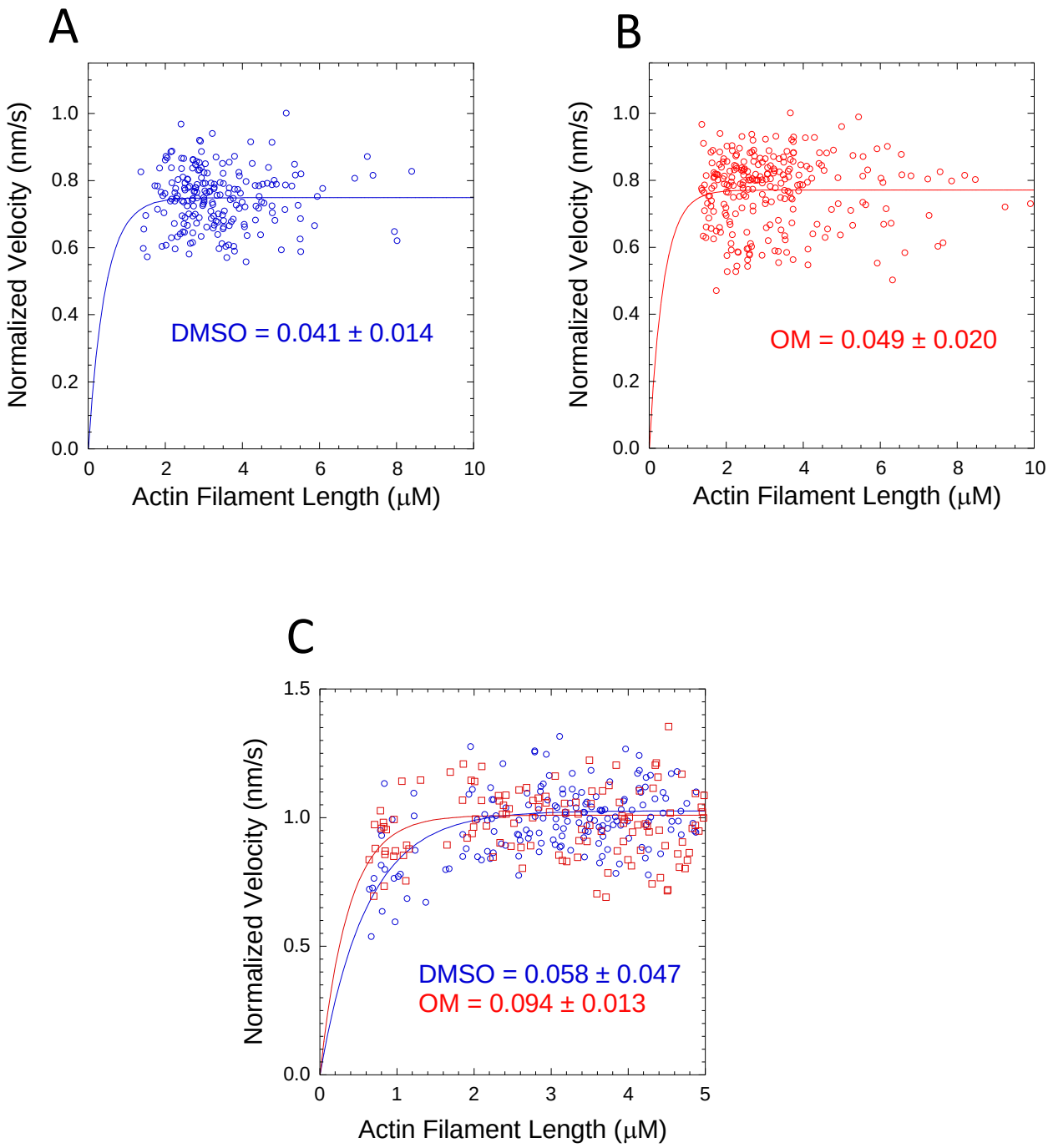

Figure 12. **<u>Measurements of Velocity as a Function of Actin Filament Length</u>**. Approximately 200 velocities and lengths for both DMSO and OM motility experiments were acquired using ImageJ software with videos examined by the NIS-Elements Viewer 4.20. Both graphs **(A)** and **(B)**, DMSO and OM respectively, are normalized velocities plotted as a function of actin filament length with a M2B-S1 concentration of 1.3μM. We also investigated length dependence at a concentration of 0.2 μM of M2B-S1 as seen in graph **(C).** A 2-fold increase in duty ratio was observed at this density.

4.5 Omecamtiv Mecarbil Effect on Human Tissue

After receiving tissue samples from the University of Kentucky Biobank, we were able to extract myosin to analyze the effects of OM on human tissue. Additionally, the patients in which these samples were extracted had received left ventricular assistive device or heart transplant or were healthy controls, but the samples were blinded. We examined the sliding velocity in the presence and absence of OM in the full length myosin from human tissue. In the absence of DMSO we found very little movement of actin filaments and the filaments that did move, moved shorter distances and at slower velocities compared to recombinant myosin samples. However, in the presence of OM most of the filaments were moving at a similar velocity to that which we determined with the recombinant cardiac myosin. The percentages of moving filaments were drastically improved from 4.96% to 90.44% in the presence of OM.

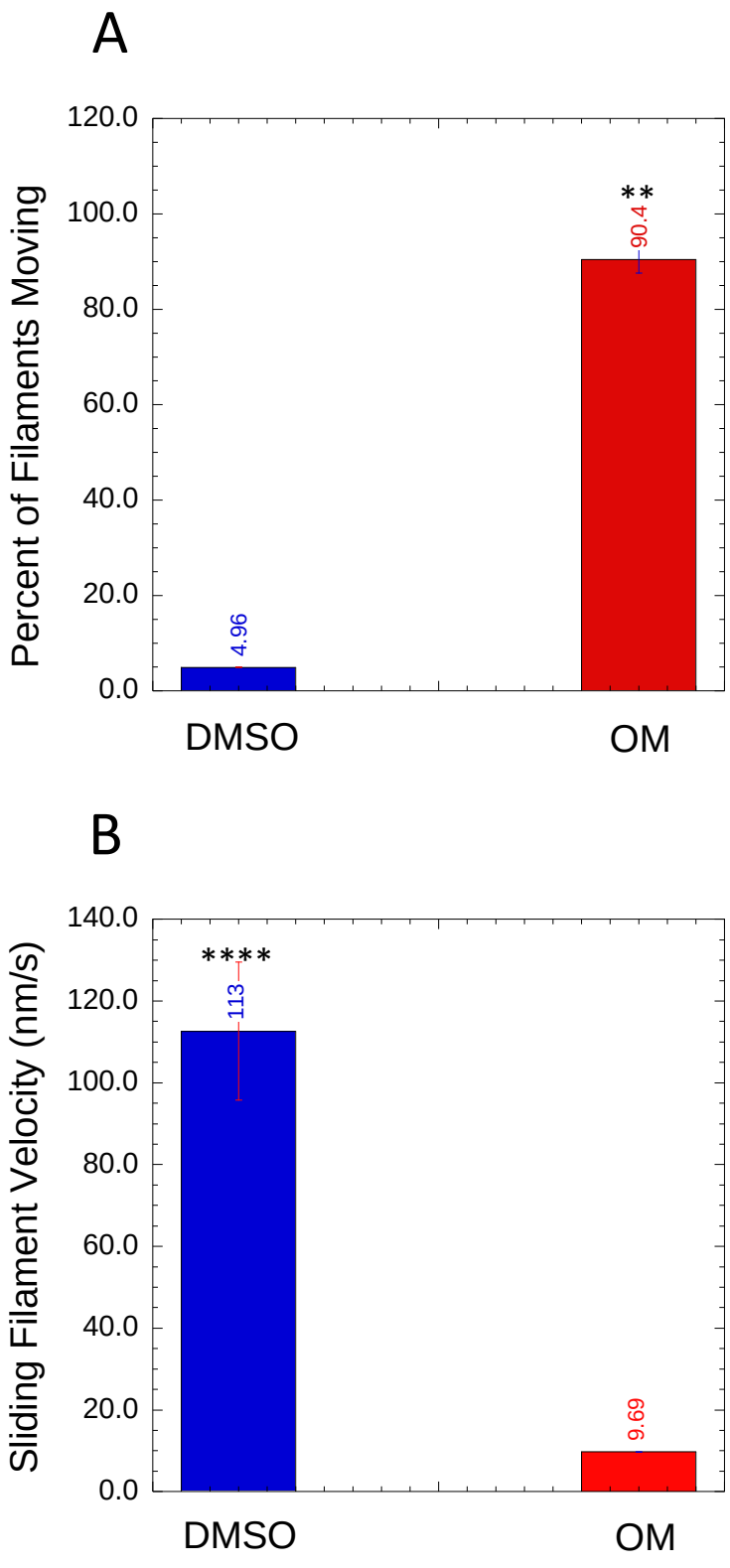

Figure 13. **The Impact of Omecamtiv Mecarbil's Effect on Human Heart Tissue**. *In vitro* motility results of purified whole cardiac myosin from three different human tissue samples which was provided by the University of Kentucky Biobank. Analysis with ImageJ software was used to examine **(A)** the total amount of filaments and the total amount of "moving" filaments in the videos in the presence of OM was greater than without OM (** $p < 0.05$) and **(B)** sliding filament velocities were higher without OM than with OM (**** $p < 0.0001$).

Chapter 5: Discussion

5.1 Introduction

Our goal of investigating the drug omecamtiv mecarbil was to determine the allosteric effect the drug has on the actomyosin interaction and how this may impact heart function in heart failure patients. OM binds directly to cardiac muscle myosin and is proposed to act as an allosteric effector to stimulate motor activity and enhance cardiac functionality without altering intracellular calcium concentrations. Our hypothesis was that OM would enhance force generation of cardiac myosin by increasing the duty ratio due to a longer attached time and enhanced force per cross-sectional area. We found that OM dramatically increases actin affinity, which slows the sliding velocity as a result of the additional drag forces associated with the enhanced affinity. *In vitro* motility and ATPase assays were performed to gain insight into changes in the functional properties of myosin in the presence of OM.

5.2 ATPase Activity

OM was shown to decrease actin-activated ATPase activity 2-fold in porcine cardiac myosin in a study performed by Liu et al in 2015. We performed ATPase assays on recombinant cardiac myosin purified from our C_2C_{12} expression system. Analysis of the ATPase activity shows that there was a 7-fold decrease in maximal activity in the presence of saturating OM (Figure 9). These results suggest that OM is not an allosteric activator but an inhibitor since the activity is diminished. However, we also observed a dramatic increase in the actin affinity as

assessed by the K_{ATPase}. The decrease in maximal ATPase rate means that OM creates a change in at least one step in the ATP cycle. Whether the change in ATP cycle is in the rate limiting step or another step that becomes rate limiting has yet to be determined. Slowing of inorganic phosphate release would slow the transition into the strongly bound state, while slowing ADP release would increase the time spent in the strongly bound state. The enhanced actin affinity suggests that the rate limiting step may be an actin attached state.

5.3 *In Vitro* Motility Sliding Velocity

In vitro motility assays were performed with cardiac myosin expressed and purified with the C_2C_{12} system. We found more than a 100-fold decrease in the sliding velocity in the presence of 10 µM OM from approximately 1500 nm/sec to 10 nm/sec (Figure 10). This is a noteworthy finding considering there is only a 7-fold decrease in maximal ATPase activity (Figure 9). If the results from ATPase and *in vitro* motility assays were directly proportional, it would suggest they have the same rate limiting step. ATPase and *in vitro* motility assays can have different rate limiting steps. For muscle myosins in the motility assay, ADP release is typically the rate limiting step, whereas phosphate release is the rate limiting step in ATPase assays (Yengo et al., 2012). The rate limiting step for β-cardiac myosin is not known but is thought to be ADP-release in ATPase assays and *in vitro* motility (Bloemink and Geeves, 2011). Thus, a major difference between the motility assay and ATPase assay is the strain dependence that can occur in the motility assay which can slow the ADP release step. Therefore, OM may make the cardiac myosin extremely sensitive to strain.

5.4 Density Dependence

Density dependence was investigated with and without OM to determine if there was a change in duty ratio. A high duty ratio myosin will be able to generate filament sliding at a constant velocity at very low densities. However, a low duty ratio myosin will decrease in velocity as a function of density. Data in Figure 11 demonstrate opposing trends when filament velocities were examined as a function of β-cardiac myosin concentration in the presence of OM and DMSO. Without the presence of OM, as the density decreases, the actin filaments are forced to travel longer distances while searching for more myosin heads to attach. In contrast, OM increased velocity as the density was decreased. We speculate that drag forces cause a decrease in the filament velocity at higher densities. These drag forces are a result of the increased affinity of the myosin heads for actin that have already generated force which resists the actin filament sliding driven by force generating myosin heads.

5.5 Length Dependence

Figure 12 illustrates that the velocity dependence on actin filament length is altered by OM. The length dependence model suggests that longer filaments would allow a greater number of myosin heads to attach and drive filament sliding. In contrast, shorter filaments would have a lower probability of interacting with myosin heads and therefore would have reduced velocities. Our results suggest there is a 2-fold increase in duty ratio which is in agreement with our results that demonstrate OM increases actin affinity. We performed our

experiments at relatively high densities which resulted in the myosin showing less sensitivity to demonstrate a change in duty ratio. However, the velocities measured at lower densities were more sensitive to changes in duty ratio which allowed us to demonstrate the difference between DMSO and OM. The observed 2-fold increase in duty ratio is still much smaller than what would be predicted from the 100-fold decrease in velocity found in the presence of OM. Thus, our results suggest there is an increase in duty ratio that would increase force production in muscle. However, there is also a large decrease in sliding velocity that could be problematic in terms of increasing function in the presence of heart failure.

5.6 Tissue Purified Compared to Recombinant

While our studies were performed on recombinant myosin expressed from a C_2C_{12}, we also examined whole myosin purified from tissue from heart failure patients provided by the University of Kentucky Biobank. Motility was not robust for whole myosin without the presence of OM; however, once OM was added, the percentage of filaments that were moving increased dramatically (Figure 13). However, there was a similar decrease in velocity in the presence of OM in comparing the expressed myosin to the tissue purified myosin. Noguchi (2003) tested isolated myosin from non-failing and failing human hearts from ventricles and atria and found that myosin motor properties are unchanged as a result of heart failure. The increase in motility observed in the presence of OM suggests that the myosin isolated from tissue was not sufficiently concentrated to generate movement, but the presence of OM enhanced the actin affinity such that movement could be generated.

5.7 Conclusion

The results we gathered in the ATPase and *in vitro* motility assays allows us to propose a model for how OM changes the force and velocity properties of cardiac muscle. We hypothesized that an increase in duty ratio would accompany the increase in actin affinity, which was supported by the length dependence experiment with low density of β-cardiac myosin. Increased actin affinity is hypothesized as a creator of drag forces which would slow velocities. Increasing the number of heads attached at different moments within the ATP cycle results in strain from attached myosin heads not producing force against those producing force. Studies should continue to attempt to obtain length dependence differences at moderate to high densities of myosin which may demonstrate more prominent differences in the duty ratio. An increase in duty ratio would suggest a mechanism for how OM increases force in a muscle fiber and determine whether the drug will be beneficial for heart failure patients. Additionally, it is also not clear how the drug changes steps within the ATP cycle which decreases velocity and ATPase activity. OM may not be beneficial because there may be a decrease in power because the large decrease in velocity may outweigh the increase in force. Given that power is the product of force and velocity, if the drug causes this decrease in velocity without increasing force we risk decreasing the power of contraction as well. Thus, the therapeutic window is critical, suggesting that OM, if beneficial physiologically, has a therapeutic level that needs to be determined to benefit heart failure patients. Future research will provide a more detailed mechanism for how OM alters cardiac myosin motor properties in a muscle fiber and in purified proteins. The results of future studies may provide crucial information about the feasibility and therapeutic dose that is recommended for OM treatment.

Bibliography:

Aksel, Tural, Elizabeth Choe Yu, Shirley Sutton, Kathleen M. Ruppel, and James A. Spudich. "Ensemble Force Changes That Result from Human Cardiac Myosin Mutations and a Small-Molecule Effector." *Cell Reports* 11.6 (2015): 910-20. *Pubmed*. Web. 2 July 2015.

Bagshaw, C. R. *Muscle Contraction*. 2nd ed. London: Chapman & Hall, 1993. Print.

Bloemink, Marieke J., and Michael A. Geeves. "Shaking the Myosin Family Tree: Biochemical Kinetics Defines Four Types of Myosin Motor." *Seminars in Cell & Developmental Biology* 22.9 (2011): 961-67. *Pubmed*. Web. 20 Dec. 2015.

Boron, Walter F., and Emile L. Boulpaep. "Organization of the Cardiovascular System." *Medical Physiology: A Cellular and Molecular Approach*. Philadelphia, PA: Elsevier Saunders, 2005. 423-46. Print.

Braunschweig, F., M. R. Cowie, and A. Auricchio. "What Are the Costs of Heart Failure?" *Europace* 13.Suppl 2 (2011): Ii13-i17. Web. 21 Dec. 2015. <http://europace.oxfordjournals.org/content/13/suppl_2/ii13>.

Chi, Qingjia, Tieying Yin, Hans Gregersen, Xiaoyan Deng, Yubo Fan, Jingbo Zhao, Donghua Liao, and Guixue Wang. "Rear Actomyosin Contractility-driven Directional Cell Migration in Three-dimensional Matrices: A Mechano-chemical Coupling Mechanism." *Journal of The Royal Society Interface* 11.95 (2014): 20131072. *Pubmed*. Web. 21 Dec. 2015.

Cleland, John Gf, John R. Teerlink, Roxy Senior, Evgeny M. Nifontov, John Jv Mc Murray, Chim C. Lang, Vitaly A. Tsyrlin, Barry H. Greenberg, Jamil Mayet, Darrel P. Francis, Tamaz Shaburishvili, Mark Monaghan, Mitchell Saltzberg, Ludwig Neyses, Scott M. Wasserman, Jacqueline H. Lee, Khalil G. Saikali, Cyril P. Clarke, Jonathan H. Goldman, Andrew A. Wolff, and Fady I. Malik. "The Effects of the Cardiac Myosin Activator, Omecamtiv Mecarbil, on Cardiac Function in Systolic Heart Failure: A Double-blind, Placebo-controlled, Crossover, Dose-ranging Phase 2 Trial." *The Lancet* 378.9792 (2011): 676-83. *Pubmed*. Web. 14 Dec. 2015.

Cruz, Enrique M. De La, and E. Michael Ostap. "Chapter 6 Kinetic and Equilibrium Analysis of the Myosin ATPase." *Methods in Enzymology Biothermodynamics, Part A* (2009): 157-92. *Pubmed*. Web. 14 Dec. 2015.

Cummings, Benjamin. "Sarcomere." *Exam 3 Review: Chapter 09: Skeletal Muscle Cell = Fiber Histology*: Addison Wesley Longman, 2001.

Dumitru, Ioana, Dr. "Heart Failure Clinical Presentation." *Heart Failure Clinical Presentation: History, Physical Examination, Predominant Right-Sided Heart Failure*. Medscape, 13 July 2015. Web. 30 Nov. 2015.

ELauzon, Anne-Marie, Dr. "In Vitro Motility Assay." *Meakins Christie Laboratories*. Quebec: McGill U, 2015.

Garcia-Pavia, Pablo, Marta Cobo-Marcos, Gonzalo Guzzo-Merello, Manuel Gomez-Bueno, Belen Bornstein, Enrique Lara-Pezzi, Javier Segovia, and Luis Alonso-Pulpon. "Genetics in Dilated Cardiomyopathy." *Biomarkers in Medicine Biomarkers Med.* 7.4 (2013): 517-33. *Pubmed*. Web. 21 Oct. 2015.

Go, A. S., D. Mozaffarian, V. L. Roger, E. J. Benjamin, J. D. Berry, W. B. Borden, D. M. Bravata, S. Dai, E. S. Ford, C. S. Fox, S. Franco, H. J. Fullerton, C. Gillespie, S. M. Hailpern, J. A. Heit, V. J. Howard, M. D. Huffman, B. M. Kissela, S. J. Kittner, D. T. Lackland, J. H. Lichtman, L. D. Lisabeth, D. Magid, G. M. Marcus, A. Marelli, D. B. Matchar, D. K. Mcguire, E. R. Mohler, C. S. Moy, M. E. Mussolino, G. Nichol, N. P. Paynter, P. J. Schreiner, P. D. Sorlie, J. Stein, T. N. Turan, S. S. Virani, N. D. Wong, D. Woo, and M. B. Turner. "Heart Disease and Stroke Statistics--2013 Update: A Report From the American Heart Association." *Circulation* 127.1 (2012): *Pubmed*. Web. 21 Dec. 2015.

Greenberg, Michael J., James D. Watt, Michelle Jones, Katarzyna Kazmierczak, Danuta Szczesna-Cordary, and Jeffrey R. Moore. "Regulatory Light Chain Mutations Associated with Cardiomyopathy Affect Myosin Mechanics and Kinetics." *Journal of Molecular and Cellular Cardiology* 46.1 (2009): 108-15. *Pubmed*. Web. 19 Nov. 2015.

Greene, Liz, Steve Henikoff, and Sharyn Endow. Digital image. *Kinesin Home Page*. Department of Cell Biology at Duke University, 25 May 2011. Web. 16 June 2015.

Harris, D.E., and D.M. Warshaw. 1993. Smooth and skeletal muscle myosin both exhibit low duty cycles at zero load in vitro. J. Biol. Chem. 268:14764– 14768.

"Heart Contraction and Blood Flow." *National Institute of Health*. National Heart, Lung and Blood Institute, 17 Nov. 2011. Web. 29 Nov. 2015.

Heart Failure Society of America, Inc. "Quick Heart Failure Facts -." *Heart Failure Society of America*. Heart Failure Society of America, 2015. Web. 5 Nov. 2015. <http://www.hfsa.org/about-hfsa/quick-heart-failure-facts/>.

Heidenreich, P. A., N. M. Albert, L. A. Allen, D. A. Bluemke, J. Butler, G. C. Fonarow, J. S. Ikonomidis, O. Khavjou, M. A. Konstam, T. M. Maddox, G. Nichol, M. Pham, I. L. Pina, and J. G. Trogdon. "Forecasting the Impact of Heart Failure in the United States: A Policy Statement from the American Heart Association." *Circulation: Heart Failure* 6.3 (2013): 606-19. *Pubmed*. Web. 21 Dec. 2015.

Huxley, A. F., and R. Niedergerke. "Structural Changes in Muscle During Contraction: Interference Microscopy of Living Muscle Fibres." *Nature* 173.4412 (1954): 971-73. *Pubmed*. Web. 11 Mar. 2015.

Kataoka, Aya, Carolyn Hemmer, and P. Bryant Chase. "Computational Simulation of Hypertrophic Cardiomyopathy Mutations in Troponin I: Influence of Increased Myofilament Calcium Sensitivity on Isometric Force, ATPase and [Ca2]." *Journal of Biomechanics* 40.9 (2007): 2044-052. *Pubmed*. Web. 21 Dec. 2015.

Kron, S. J., and J. A. Spudich. "Fluorescent Actin Filaments Move on Myosin Fixed to a Glass Surface." *Proceedings of the National Academy of Sciences* 83.17 (1986): 6272-276. *Pubmed*. Web.

Liu, Yingying, Howard D. White, Betty Belknap, Donald A. Winkelmann, and Eva Forgacs. "Omecamtiv Mecarbil Modulates the Kinetic and Motile Properties of Porcine β-Cardiac Myosin." *Biochemistry* 54.10 (2015): 1963-975. *Pubmed*. Web. 8 Dec. 2015.

Malik, F. I., J. J. Hartman, K. A. Elias, B. P. Morgan, H. Rodriguez, K. Brejc, R. L. Anderson, S. H. Sueoka, K. H. Lee, J. T. Finer, R. Sakowicz, R. Baliga, D. R. Cox, M. Garard, G. Godinez, R. Kawas, E. Kraynack, D. Lenzi, P. P. Lu, A. Muci, C. Niu, X. Qian, D. W. Pierce, M. Pokrovskii, I. Suehiro, S. Sylvester, T. Tochimoto, C. Valdez, W. Wang, T. Katori, D. A. Kass, Y.-T. Shen, S. F. Vatner, and D. J. Morgans. "Cardiac Myosin Activation: A Potential Therapeutic Approach for Systolic Heart Failure." *Science* 331.6023 (2011): 1439-443. *Pubmed*. Web. 20 Apr. 2015.

Mamidi, Ranganath. "Molecular Effects of the Myosin Activator Omecamtiv Mecarbil on Contractile Properties of Skinned Myocardium Lacking Cardiac Myosin Binding Protein-C." *Journal of Molecular and Cellular Cardiology* 85 (2015): 262-72. 19 June 2015. Web. 8 Dec. 2015.

Mayo Foundation for Medical Education and Research. "Chambers and Valves of the Heart." - *Mayo Clinic*. Web. 20 Dec. 2015.

McPhee, Stephen J. "Cardiovascular Disorders: Heart Disease." *Pathophysiology of Disease: An Introduction to Clinical Medicine*. Stamford, CT: Appleton & Lange, 1997.

Milgrom-Hoffman, M., Z. Harrelson, N. Ferrara, E. Zelzer, S. M. Evans, and E. Tzahor. "The Heart Endocardium Is Derived from Vascular Endothelial Progenitors." *Development* 138.21 (2011): 4777-787. *Pubmed*. Web. 21 Oct. 2015.

Nagy, L., Á Kovács, B. Bódi, E. T. Pásztor, G. Á Fülöp, A. Tóth, I. Édes, and Z. Papp. "The Novel Cardiac Myosin Activator Omecamtiv Mecarbil Increases the Calcium Sensitivity of Force Production in Isolated Cardiomyocytes and Skeletal Muscle Fibres of the Rat." *British Journal of Pharmacology Br J Pharmacol* 172.18 (2015): 4506-518. *Pubmed*. Web. 14 Dec. 2015.

National Center for Chronic Disease Prevention and Health Promotion, Division for Heart Disease and Stroke Prevention. "Heart Failure Fact Sheet." *Centers for Disease Control and Prevention*. Centers for Disease Control and Prevention, 30 Nov. 2015. Web. 21 Dec. 2015. <http://www.cdc.gov/dhdsp/data_statistics/fact_sheets/fs_heart_failure.htm>.

Noguchi, T. "Myosin from failing and Non-failing Human Ventricles Exhibit Similar Contractile Properties." *Journal of Molecular and Cellular Cardiology* 35.1 (2003): 91-97. *Pubmed*. Web. 22 Mar. 2015.

Rosse, Cornelius, Penelope Gaddum-Rosse, and W. Henry Hollinshead. "The Pericardium, the Heart, and the Great Vessels." Hollinshead's Textbook of Anatomy. 5th ed. Philadelphia, PA: Lippincott-Raven, 1997. 463-94. Print.

Schwartz, Robert S., Hugh Watkins, Houman Ashrafian, and Charles Redwood. "Inherited Cardiomyopathies." *New England Journal of Medicine N Engl J Med* 364.17 (2011): 1643-656. *Pubmed*. Web. 20 Mar. 2015.

Sivaramakrishnan, Sivaraj, Euan Ashley, Leslie Leinwand, and James A. Spudich. "Erratum: Insights into Human β-Cardiac Myosin Function from Single Molecule and Single Cell Studies." *Journal of Cardiovascular Translational Research J. of Cardiovasc. Trans. Res.* 4.1 (2010): 114. *Pubmed*. Web. 14 Dec. 2015.

Spudich, James A. "Hypertrophic and Dilated Cardiomyopathy: Four Decades of Basic Research on Muscle Lead to Potential Therapeutic Approaches to These Devastating Genetic Diseases." *Biophysical Journal* 106.6 (2014): 1236-249. *Pubmed*. Web. 28 Mar. 2015.

Standring, Susan, Neil R. Borley, and Henry Gray. "Heart and Great Vessels." Gray's Anatomy: The Anatomical Basis of Clinical Practice. 14th ed. London: Elsevier, 2008. 959-87. Print.

Stewart, Simon, Kate Macintyre, David J. Hole, Simon Capewell, and John J.v. Mcmurray. "More 'malignant' than Cancer? Five-year Survival following a First Admission for Heart Failure." *European Journal of Heart Failure* 3.3 (2001): 315-22. *Pubmed*. Web.

Teerlink, John R., Cyril P. Clarke, Khalil G. Saikali, Jacqueline H. Lee, Michael M. Chen, Rafael D. Escandon, Lyndsey Elliott, Rachel Bee, Mohammad Reza Habibzadeh, Jonathan H. Goldman, Nelson B. Schiller, Fady I. Malik, and Andrew A. Wolff. "Dose-dependent Augmentation of Cardiac Systolic Function with the Selective Cardiac Myosin Activator, Omecamtiv Mecarbil: A First-in-man Study." *The Lancet* 378.9792 (2011): 667-75. *Pubmed*. Web. 14 Dec. 2015.

Texas Heart Institute. "Inotropic Agents - Texas Heart Institute Heart Information Center." *Texas Heart Institute Heart Information Center*. July 2015. Web. 30 Nov. 2015.

Winkelmann, Donald A., Eva Forgacs, Matthew T. Miller, and Ann M. Stock. "Structural Basis for Drug-induced Allosteric Changes to Human β-cardiac Myosin Motor Activity." *Nature Communications Nat Comms* 6 (2015): 7974. *Pubmed*. Web. 22 October 2015.

Yang, Jian, Wei-wei Xu, and Shen-jiang Hu. "Heart Failure: Advanced Development in Genetics and Epigenetics." BioMed Research International 2015 (2015): 352734. PMC. Web. 6 Nov. 2015.

Yengo, Christopher M., Yasuharu Takagi, and James R. Sellers. "Temperature Dependent Measurements Reveal Similarities between Muscle and Non-muscle Myosin Motility." *J Muscle Res Cell Motil Journal of Muscle Research and Cell Motility* 33.6 (2012): 385-94. Web.